Study on the Characteristics of Tropical Cyclones in the Southwest Pacific

TAUVALE, Luteru Agaalii

A dissertation for the degree of Doctor of Science

Department of Earth and Environmental Science

Graduate School of Environmental Studies, Nagoya University

2020

Abstract

Tropical cyclones (TCs), some of the most influential weather events on the planet and can have severe impacts to people and places on the Southwest Pacific. Therefore, determination of long-term TC variability in the region is very timely and relevant. However, changes in TC activity region specific, are poorly understood and is a topic that has been relatively infrequently studied to date. This is due mainly to the discrepancies among the various datasets and the very limited instrumental records. This study explores the relative long-term changes in the variability of the Southwest Pacific tropical cyclones.

The first half of the study is focused on the geographic and meteorological characteristics of 479 tropical cyclones (TCs) in the Southwest Pacific (5°–35°S, 135°E–120°W) from 1970 to 2017 by using the latest Southwest Pacific Enhanced Archive of TCs dataset. Here we show, various TC characteristics on the basis of selected metrics such as the TCs' geographic distributions, numbers, intensities, length in days (TC days), accumulated cyclone energy (ACE), and power dissipation index (PDI). Correlation analyses were conducted to determine the association of these metrics with the risen sea surface temperature in the region. An increasing behavior of TC activities has been revealed in the western, northwestern, northern, and central subdomains of the nine subdomains in the study domain. The average latitudinal location where TC genesis and maximum intensity occurred remained almost stable over time. TCs are more often than not move in the southward to southeastward direction, and most reached their maximum intensities in the western and central parts of the study domain. Annually, the number of TCs and TC days decreased while the numbers of stronger TCs slightly increased, and stronger TC days increased. Intensity metrics such as the highest annual lifetime-maximum intensity and average annual lifetime-maximum intensity also increased. The highest annual

maximum intensification rates show no obvious change over the study period, nor did ACE and PDI. The results show correlations between the highest annual lifetime-maximum intensity and average sea surface temperature (SST) variations, as well as correlations between TC days and average SST variations in the region. This suggests that SST has some linkage on the lifetime-maximum intensity and TC days while status of association with other metrics is less clear.

The latter part of the study was to examine the intensifying location of TCs, and the time change of their average in the area defined by 5°–35°S, 155°E–120°W from 1982 to 2017. A total of 282 TCs with 1636 intensifying events and 352 rapidly intensifying events were examined. From the analyses, it appears to be preferred latitude for TC intensification, in the confines of around 10-20°S latitude band. However, when events are grouped into 5° latitude intervals, the 15-20°S band has the greatest number of events. Analyses of long-term observed trends indicated that the number of intensifying events has decreased by roughly 20% per 10 years while rapidly intensifying events has exhibited an increase of roughly 15% per 10 years. There is some evidence that the average latitude where tropical cyclones intensify has been migrated poleward. In contrast, a clear equatorward movement appears evident for rapidly intensifying events. There are clear implications that the poleward migration of intensifying latitude of all intensifying events are occurring concurrently with the poleward expansion of warmer SST. Isotherms of higher SST migrate southward more rapidly. This indicates that the high SST over the equatorial side have extended poleward and at the same time, region where intensifying events occur frequently is becoming warmer with time.

In summary, the research significantly enhanced and improved our understanding of the characteristics of TC activity in the Southwest Pacific; particularly with respect to the continuing warming climate; and it emphasized the necessity for determination of long-term past TC

activity and may also facilitate improved future projections. In addition, this research can be served as a baseline study to aid in the ongoing researching efforts on TCs in the Southwest Pacific. And for a data sparse and understudies' region like the Southwest Pacific, it is necessary to carefully consider the quality of dataset to be used, thereby enabling the provision of more robust results.

Keywords

tropic cyclones; Southwest Pacific; SPEArTC; sea surface temperatures; interannual variability; long-term trends; intensifying location; poleward migration; climatology.

List of Contents

1. Introduction

1.1 Tropical Cyclones

Tropical Cyclones (TCs) are perhaps, amongst the mostly deadly and destructive natural hazard on the planet. They can generate severe weather, including extreme winds, heavy rainfall, intense storm surge flooding, and tornadoes, for extended periods over relatively large spatial areas. Here, TC, also known as 'Cyclone' is a generic term used by the World Meteorological Organization (WMO) to define non-frontal synoptic scale low pressure systems in which the surface winds equal or exceed the minimum of 34 knots (World Meteorological Organization 2016). Depending on their geographical locations and intensities, cyclones are called by other terms across the world. For example, in the northern hemisphere, the terms 'hurricane' and 'typhoon' are often used for tropical cyclones to east (United States) and west (Asia) of the International Dateline respectively, while Southern Hemisphere stick to the tern tropical cyclone.

According to Gray (1968, 1977), the six primary parameters necessary for TC genesis are low level vorticity, Coriolis parameter, vertical wind shear, ocean thermal energy, relative humidity and conditional instability. These widely accepted parameters are generally favorable over tropical or subtropical warm oceans. Globally, there are seven identified TC prone regions, four in the Northern hemisphere and three in the Southern Hemisphere including the Southwest Pacific (World Meteorology Organization 2017).

1.2 Southwest Pacific current exposure and vulnerability to TCs

The Southwest Pacific region corresponds to the area defined by 135°E, 120°W, equator and 50°S. Apart from the landmasses of Australia and New Zealand, the Southwest Pacific region contain scores of small island nations and territories, which range in size from small coral atolls to volcanic islands of few hundred square kilometers surrounded by ocean. According to World Bank (2006, 2013), TCs are the most dangerous form of natural disaster which account for 76% of disasters within the region, resulting in economical damage and casualties enormously. Annually, an average of 11-13 TCs form in the region, with 2-4 attaining major TCs status (Diamond et al. 2013; Magee et al. 2016). The most recent costly catastrophes include Category (Cat) 5 Cyclone Pam that affected the Vanuatu islands in 2015 costing over $USD449.9 million (Government of Vanuatu 2015), Cyclone Winston (Cat 5) that landed in the Fiji islands in 2016 with an estimated economic value of $USD0.9 billion (Government of Fiji 2016) and Cyclone Gita (Cat 5) that affected the Tongan islands in 2018 with an estimated cost at over $USD164.1 million (Government of Tonga 2018). Isolation, fragile infrastructure, slow economic growth, unfavorable shoreline to land area ratio and the dependence on subsistence farming are some of the regional-wide manifestation that have exacerbated the vulnerability of most of the island nations and territories in the region (Barnett 2001; Magee and Verdon-Kidd 2018). Moreover, the increased human settlements along the low-lying coastal areas where TC usually struck has also led to high monetary impacts.

Several studies have projected the future TC activity and view it as a phenomenon due to the effect of climate change. For example, a future increase in TC intensity in terms of precipitation (Gualdi et al. 2008), increase in maximum wind speed (World Bank 2013) and increase in the frequency of intense TCs (Oouchi et al. 2006; Murakami and Sugi 2010).The

combination of such future projections with previous severe disaster records, and some of the then-present observational studies (discussed next section), emphasized a heightened risk for the region in response to rising sea surface temperatures over time in tandem with enhanced greenhouse conditions (Emanuel 2005; Knutson and Tuleya 2008; Terry and Gienko 2010). It is felt that, more comprehensive long-term variability studies of TC activity are of great importance to unravel the specific behavior of these events so timely and relevant estimations can be made of their impacts on human activities and for future climate prediction. An ability to design appropriate cost-effective mitigation measures in advance for these regional TC impacts depends on an understanding of the key controlling factors that drive their (TCs) variability.

1.3 Research activities in the Southwest Pacific

To date, there have been a few TC related studies undertaken, documenting TC activity in the past for the Southwest Pacific region. These earlier attempts are all considered here, providing sufficient understanding leading up to this study.

Basher and Zheng (1995) documented the relationship between TC number and Southern Oscillation Index (SOI), in the South Pacific (10-20°S, 150°E-130°W) using the New Zealand Meteorological Service TC information from 1969 to 1989. They found a marked influence of sea surface temperature (SST) and Southern Oscillation (SO) phase to TC numbers' spatial variations. Nicholas et al. (1998) found strong a declined in TC numbers since 1969 and a slightly increased in the number of more intense TCs in the Australian region (south of the equator, 105-160°E) which has been largely attributed to El Niño Southern Oscillation (ENSO) phenomenon.

A detailed analysis of characteristics of TCs in the Australian region were produced by Dare and Davidson (2004). In their study, they identified the northeastern region around the coastline (145-155°E) and the Gulf of Carpentaria as main TC genesis focused areas based on 40 seasons of satellite-supported observations from 1963 to 2002. Based on data from numerous historical sources (including peer-reviewed publications, newspapers, sea-faring observations and other media reports dating back to the 1900s), Callaghan and Power (2011) found a statistically significant declined in the number land-falling TCs in eastern Australia (~16-28°S, ~145-153°E), however the reason for such trend remains unclear.

Chand and Walsh (2009) used the Joint Typhoon Warning Center (JTWC) best-track data to explore the interannual variability of TC tracks in Fiji-Samoa-Tonga (FST) region (5-25°S,170°E-170°W) from 1970 to 2006. They found that TC activity is strongly modulated by the ENSO, whereby El Niño (La Nina) conditions led to more (less) TCs, and TC genesis locations are well correlated with large-scale environmental parameters such as vertical wind shear, 200hPa atmospheric divergence and 850hPa cyclonic relative vorticity. Using the accumulated cyclone energy (ACE) as a measure of TC intensity, Chand and Walsh (2011), found that over in the same FST region, equatorward of 15°S, ACE values are above average during the warmer (El Niño) phase when TCs retain their strength for a longer period of time, compared with cooler (La Niña) counterpart. The reverse is true for the regions in poleward of 15°S. Iizuka and Matsuura (2012) reported similar relationships, whereby El Niño produce more TCs over the northeastern quadrant of the Southwest Pacific while decrease during La Niña.

Vincent et al. (2009) used the European Medium-Range Weather Forecast (ECMWF) Re-analysis (ERA40) to assess the interannual variability of the South Pacific Convergence Zone (SPCZ) and its influence on TC genesis in the South Pacific (0-30°S,140°E-120°W) from 1979

to 2002. They found that SPCZ which is a major cyclogenesis area, is strongly modulated by the ENSO phenomenon.

These studies listed above (and others referred to in this study) has undoubtedly provide a good understanding of the characteristics of TC in the region. But still, TC activities has been studied far less in comparison to other TC regions generally due to sheer vastness and low population density, limited amount of meteorological observational data (sparse open ocean) and lack of homogenous TC information dataset (Diamond et al. 2012). As we progress with time, climate scientists have identified and have questioned the suitability of TC dataset that have been used to conduct global TC studies on the grounds of data quality. Some of these concerns are well discussed in the existing literature.

1.4 TC data quality and reliability

Webster et al. (2005) reported a large increased in the global number of intense Cat 4 and 5 hurricanes from 1970 to 2004. They have attributed their findings to the to increasing SSTs in various ocean basins globally. Klotzbach (2006) examined the trends of net TC activity from 1986 to 2005 and found that, there has been small increase in global Cat 4 and 5 hurricanes, despite the increased in SST. Klotzbach (2006) stated that the small positive trend in their findings is most likely due changing observing system and analysis practices in the later part of the study period (1996-2005). The sensitivity of TC maximum winds estimation to these improvements has been explained by Landsea et al. (2006). Klotzbach and Landsea (2015) revisited the study of Webster et al. (2005) and with additional 10 years of data, they found a small insignificant decreasing trend in the number of Cat 4 and 5 hurricanes, particularly

between 1990 and 2014. Klotzbach and Landsea (2015) argued that, the increasing trends reported by Webster et al. (2005) are artificial and may have been influenced by the quality of TC historical dataset, particularly around the period 1970s and 1980s whereby data certainty decrease backwards in time.

The main source of TC information globally comes from surface and upper air in situ observations, aircrafts reconnaissance and satellites. However, TC spend most of their lifetime over the ocean where in situ observations are very limited. Satellites observations were introduced in the early 1960s and has proven to be more effective in TC observations and monitoring thereafter (Velden et al. 1998). The satellite-based Dvorak Technique (and subsequent refinement versions) has become the main readily used operational tool for estimating TC intensities globally since the early 1970s (Dvorak 1972, 1975, 1984, Knaff et al. 2010). This technique, derived TC intensities by applying a pattern recognition scheme and such technology have led to a significant improvements of TC intensity estimates (Kossin et al. 2013). Most designated WMO Regional Specialized Meteorological Centers and Tropical Cyclone Warning Centers have consistently used the Dvorak technique since the late 1980s (Knaff et al. 2010). Due to the fact that the Dvorak Technique does not measure TC intensity directly, its application is subjective to decision making and it is common to have significantly different intensities estimate by different operational centers, or between specialists on the basis of identical information (Landsea et al. 2006; Kossin et al. 2013).

In the South Pacific, the absence of satellite observations prior to the 1980s, TCs that never approached land or encountered a ship had a greater chance of been undetected and thus the real TC number, tracks and intensities may never be known (De Scally 2008). Moreover,

being a largely ocean dominated region means only a few surface observations are available on small islands and from buoys. Similarly, Holland (1981) suggested that TC data prior to the 1960s in the Australian region were largely inconsistent and incomplete due to lack of surface observations and monitoring such as regular aircraft reconnaissance. Holland further stated that the 1960/70 is the first reliable year, attributable to the availability of geostationary satellite imageries.

While observation and monitoring improvements are evident in the existing literature, it is obvious that these aforementioned studies and considerable debates have clearly highlighted the need for the development of then-current reliable records of TC activity. It is believed that such development will boost observational based TC studies to be reliably conducted by the research community.

1.5 Brief overview of best-track datasets in the Southwest Pacific

The term "best track" specifically refers to the best estimate of the storm's position and intensity on a 6-hr basis (typically at 00, 06, 12 and 18UTC). Best track data are compiled after the end of TC seasons using all the available information which included direct surface and upper air observations, remote sensing from satellites and other platforms. The best-tracking practices include many agencies and estimates may vary from one agency to another.

Best-track data are the basis for various observational based TC related studies. There is number of available existing TC best-track datasets that span the Southwest Pacific region. These datasets include the Joint Typhoon Warning Center (JTWC) dataset (Chu et al. 2002),

International Best Track Archive for Climate Stewardship (IBTrACS, Knapp et al. 2010; Kruk et al. 2010), Australia Bureau of Meteorology National Climate Center (BOM NCC) dataset (Trewin 2008), the recent Southwest Pacific Enhanced Archive of Tropical Cyclones (SPEArTC, Diamond et al. 2012) and others. Most of the existing TC studies in the region are generally based on these datasets. Full details of these existing datasets and their spatiotemporal coverage are explained in the study of Magee et al. (2016).

The development of the SPEArTC in 2011/2012 is believed to have united, re-secured and centralized data from multiple sources, making it available at convenient formats (Diamond et al. 2012). The SPEArTC is based on the IBTrACS database plus new information recovered from archive of Pacific Island Nations Meteorological Services (PINMS). The developers have high confidence level that SPEArTC is so far, the most comprehensive, more holistic and quality-controlled repository of TCs for the Southwest Pacific in comparison to alternative best-track counterparts. The SPEArTC dataset will be discussed in greater depth in the data section.

A spatio-temporal intercomparison between the JTWC, IBTrACS and SPEArTC was provided by Magee et al. (2016) for the Southwest Pacific region (0-35°S,135°E-120°W). The JTWC and IBTrACS are generally the most used TC best-track datasets by researchers worldwide. Out of the three datasets been examined, it was determined that SPEArTC was the most complete and/or accurate dataset. To date, the used of SPEArTC for TC related studies in the region is widespread (e.g., Diamond et al. 2013; Blunden and Arndt 2016, 2017; Hoarau et al. 2018; Magee and Verdon-Kidd 2019). Therefore, it is an opportune time, to optimize this new repository to explore the climatological characteristics and fluctuations of observed TC activity.

The lead up to the current study is generally based on the positive outcomes from these prior studies as mentioned earlier, specifically in the selection of the dataset, spatial extent and time periods. The author believes that, taking such information into consideration would better characterize the characteristic of TCs in the region.

1.6 Objectives of the study

The overarching aim is to provide a broad assessment and/or an up to date comprehensive study which should better understand the spatio-temporal characteristics of TC activity in the Southwest Pacific (defined by 5-35°S, 135°E-120°W). The objectives to achieve this are (1) identify the best suitable and/or reliable dataset for such analysis, (2) apply the dataset to the chosen most suitable TC metrics, that should best represent the behavior of TCs in the region, (3) explore the similarities and dissimilarities with similar prior studies, and (4) draw conclusions to reflect the then-current state of TC activity in the region. In addition, attempts were also been made to discover any link between TC metrics variability and the changes in the background SST.

It is expected that the study can be used as a guidance to improve TC outlooks, increase the scientifically peer reviewed literature on TCs in the region, and serving as baseline for similar related studies in the future. Furthermore, it is hoped that the study, or part of it is eligible for inclusion in future Intergovernmental Panel on Climate Change (IPCC) Assessment Reports (ARs) to strengthen regional capacities' engagements with the IPCC process. IPCC ARs are important technical resources worldwide which contains knowledge of past, current and future climate based on sound, peer-reviewed science. Its application is in the realm of informing negotiations, policy making and Council of Parties (COP) dialogues (IPCC Secretariat 2013).

2. Data

The two different types of data used in this study are TC best track data and Sea Surface Temperature data. These datasets are freely available via internet.

2.1 Best-track data

The TC data in this study was obtained from the best-track of the SPEArTC (Diamond et al. 2012). Here, a brief explanation of the dataset is provided and refer the interested reader to the original reference for full details. SPEArTC contains information of TCs originating in the region encompassed by 5-65°S, 135°E-120°W) from 1840 to present. The dataset consist of TC Name, latitude and longitude position of the TC center, minimum sea level pressure (MSLP), and maximum (10-min average) sustained near surface wind speed, which observed at 0000, 0600, 1200 and 1800 Coordinated Universal Time (UTC). Because the TC season in the Southern Hemisphere spans the calendar years, the TC year in the dataset (and this study) is label with the latter year; for example, the TC season starting in October 2016 and ending in April 2017 is referred to as the 2017 TC year. Because SPEArTC incorporate data from many sources, a quality control procedure was employed by the developers, leading to the additional (subtraction) of new (duplicate) tracks. The SPEArTC dataset us updated at the end of every TC season and is freely available at Asia-Pacific Data Research Center website (http://apdrc.soest.hawaii.edu/projects/speartc/resources.php).

2.2 Sea surface temperature data

Two sets of Sea Surface Temperature were used in this study. The first dataset was obtained from the Extended Reconstructed Sea Surface Temperature archive, version 5 (ERSSTv5, Huang et al. 2017). ERSSTv5 is a globally monthly from the U.S National Oceanic and Atmospheric Administration (NOAA), with a horizontal resolution of 2° × 2° latitude-longitude and are available for the period extending from January 1854 to the present. The dataset contains SST anomalies computed with respect to the 1971-2000 monthly climatology as a baseline to depict change. The SST data are available at the National Centers for Environmental Information website (https://www.ncdc.noaa.gov/data-access/marineocean-data/extended-reconstructed-sea-surface-temperature-ersstv5).

The second SST dataset was obtained from the NOAA Daily Optimum Interpolation Sea Surface Temperature (or daily OISST) dataset (Reynolds et al. 2007). The OISST has a horizontal resolution of 0.25° × 0.25° latitude-longitude on a global grid (1440 × 720) and its available from late 1981 to the present. The SST data are available at the National Centers for Environmental Information website (https://www.ncdc.noaa.gov/oisst/data-access).

3. Methodology and definitions

3.1 Characteristics of TCs from 1970 to 2017

3.1.1 Domain and time period

The main study area referred hereafter as Southwest Pacific corresponds to the region extending from 5 to 35°S and 135°E to 120°W (Fig. 1). The current domain is slightly different from the WMO official domain of the Southwest Pacific, which delimited in the west by 160°E. The domain is extended to the west to include TCs that formed west of 160°E before spending most of their lifetime in the WMO official domain (Diamond et al. 2012). TCs beyond 35°S are excluded because it is likely that some of these storms have undergone extra-tropical cyclone transition and have lost their TC characteristics. The main domain was sub divided geographically into nine subdomains (refer Fig. 3c), named northwest (NW), north (N), northeast (NE), west (W), central (C), east (E), southwest (SW), south (S), and southeast (SE), enabling specific subdomain analyses where necessary, which is important, given significant variation in TC activity across the region (Magee and Verdon-Kidd 2019).

Because of data deficiencies before the 1970s (pre-satellite era), this study is restricted to the period extending from 1970 onward, which is considered to be the most reliable period owing to the influx of satellite observations in the region (Holland 1981; Goebbert and Leslie 2010; Terry and Gienko 2010). Involving the pre-satellite era has often complicated earlier detection and attribution variability TC studies in the region (Dare and Davidson 2004; Hassim and Walsh 2008; Haig et al. 2014). Thus, the chosen period is believed to have somehow avoided the surrounding issues related to the quality of records before the satellite era.

In accordance with WMO's definition of TCs for the South Pacific and Southeast Indian Ocean (World Meteorological Organization 2016), only TCs designated as in a tropical phase with wind speed *V* equal or exceed the minimum of 34 knots are considered TC in this study. Because *V* is commonly used to define TC intensity in most prior studies, this study does so for consistency and also, *V* is generally more complete in SPEArTC than sea level pressure. Moreover, destructive potential of TCs is better related to the metric *V* (Emanuel 2005; Knaff and Zehr 2007), such as damage to buildings and infrastructure (Guard and Lander 1999; Stewart 2003; Ginger et al. 2007) in comparison to MSLP.

3.1.2 Geographic distribution of TCs

Firstly, analyses are focused on the spatial distribution of location of TC genesis, location where TC reach its peak intensity and the paths of TCs on a decadal basis. The study then attempts to examine the annual changes in the average latitude of TC genesis and the average latitude of TC lifetime maximum intensity. The target here has been placed on identifying regional spatial and temporal patterns in the aforementioned metrics over time. In this study the location of TC genesis is defined as the location at which the intensity first reached $V \geq 34$ knots. The location of TC maximum intensity, LV_{max} hereafter, is the location where the TC first attained its lifetime-maximum intensity (V_{max}) over the course of its life and at least 6 hours after genesis.

3.1.3 TC numbers

A tropical system is counted as a TC if its *V* reaches at least 34 knots. Because of the different impacts associated with different intensity scale, weak and intense TCs were also analyzed separately. Here the analyses were focused on all TCs, weak TCs and intense TCs. A threshold *V* of 86 knots was used to isolate weak and intense TCs. In the Southwest Pacific, TCs with $V \geq 86$ knots correspond to severe Cat 4 and Cat 5 TCs. TCs with such strength are typically the most dangerous categories in terms of high winds related impacts and are responsible for vast majority of destruction worldwide (e.g. Pielke et al. 2008). A very similar threshold was used in some of the previous studies that we referred to in the present study (e.g. Webster et al. 2005; Hoarau et al. 2018) to classify weak and intense TCs. For simplicity, weak and intense TCs are referred to here as weaker TCs ($V < 86$ knots) and stronger TCs ($V \geq 86$ knots), respectively.

3.1.4 TC intensity

Intensity is a measure of extreme meteorological conditions which is commonly measure by the maximum near surface wind speed and/or MSLP. Despite MSLP being the more accurate intensity measure, TC intensity in this study is represented by *V*, the maximum (10-min average) sustained near-surface wind speed, for reasons explained in subsection 3.1. Here, the lifetime-maximum intensity, V_{max}, is defined as the maximum value of *V* throughout the lifetime of each TC. The highest V_{max} of all TCs in each year is expressed as $\hat{V}_{max}$ and defined by

$$\hat{V}_{max} = \mathrm{Max}\left(V_{max,i}\right), \quad (1)$$

where $V_{max,i}$ is the lifetime-maximum intensity of individual TC*i* in knots.

The average maximum intensity of all TCs in each TC season is referred to hereafter as $\bar{V}_{max}$ and is defined by

$$\bar{V}_{max} = \frac{\sum_{i=1}^{N} V_{max,i}}{N}, \quad (2)$$

where *N* is the number of TCs in each TC season.

The study also examined the intensification aspects of TCs with more emphasis placed on the annual variation in the maximum intensification rate (IR_{max}). The rate at which a TC change its intensity from time to time remains a challenge to many operational forecasters, especially when a sudden change occurs (Rappaport et al. 2009), given its potentially catastrophic impact on unprepared coastal communities. Here, the intensification rate of a TC at a given time is defined as the increase in V_{max} over a 6 h period. The IR_{max} is the lifetime-maximum rate of change in the intensity of a particular TC and is defined by

$$IR_{max} = Max\left(\frac{\Delta V}{\Delta t}\right) = Max\left(\frac{V_n - V_{n-1}}{t_n - t_{n-1}}\right), \quad (3)$$

where t is the observation time and n is an index of time. The highest IR_{max} in each year, $\widehat{IR}_{max}$, is defined by

$$\widehat{IR}_{max} = \text{Max}\left(IR_{max,i}\right), \quad (4)$$

where $IR_{max,i}$ is the lifetime-maximum intensification rate of individual TC*i* in knots per hour.

3.1.5 TC days

Since TC pose a major risk, its duration is one of the most important information that people in the affected regions want to know. Roughly speaking, the longer the TC duration, the

more damage could be done as a consequence. In this study, TC duration is referred to as TC Days which is defined as the total number of days when a storm sustains TC intensity (Webster et al. 2005; Frank and Young 2007). The annual number of TC days is the sum of all TC days within each season,

$$\text{TC days} = \frac{1}{24}\sum_{i=1}^{N}\sum_{n=2}^{M_i}\left(t_{i,n} - t_{i,n-1}\right), \quad (5)$$

where $t_{i,n} - t_{i,n-1}$ is the time difference of two observations in hours, M_i is the number of observations in each TC and the summation is divided by 24 to convert from hours to days.

3.1.6 Accumulated cyclone energy

ACE is an integrated TC metric that convolves intensity and duration over the lifetime of a TC (Bell et al. 2000). Such quantity is related to the kinetic energy of a TC and has been widely used in studies to examine TC activity (e.g. Camargo and Sobel 2005; Chand and Walsh 2011; Villarini and Vecchi 2013; Corporal-Lodangco et al. 2016; Zhang et al. 2016). In this study, ACE is therefore, estimated as the sum of the squares of *V* every 6 h interval (usually measured at 0000, 0600, 1200, and 1800 UTC) throughout the lifetime cycle of a TC. ACE totals for each year are obtained as an annual accumulation from

$$\text{ACE} = \sum_{i=1}^{N}\sum_{n=1}^{M_i} {V_{i,n}}^2, \quad (6)$$

where $V_{i,n}$ in m s^{-1} is defined every 6 h for each TC. The unit of the ACE is $m^2\ s^{-2}$ which is equivalent to J kg^{-1} and the latter is used in this paper.

3.1.7 Power dissipation index

Similar to the ACE, the power dissipation index (PDI) metric is one of the available integrated quantities to measure TC activity. PDI has been used worldwide by researchers to assess the associated power and destructiveness of TCs (Emanuel 2007; Murakami et al. 2014; Li et al. 2017). Based on the sum of the cube of *V* over the TC lifespan (Emanuel 2005), the annual PDI is defined by

$$\mathrm{PDI} = \sum_{i=1}^{N} \sum_{n=1}^{M_i} {V_{i,n}}^3 . \qquad (7)$$

Units of *V* converted are converted from knots to m s^{-1} (1 knot ≈ 0.51 m s^{-1}) only for the calculations of the integrated TC intensity metrics such as ACE and PDI reflecting the proportionality of wind velocity to energy and power respectively.

3.1.8 Trends and correlation analyses

Linear model using regression analysis which is based on the best possible fit were added to the time series of the variables to show their observed trend. Correlation-based analyses was also used as a statistical measure to explain the magnitude of linear association between variables. In this study the strength of such relationships is determined by the well-known coefficient of determination (r^2) statistic and characterized as very strong (r^2 = 0.8–1.0), strong (0.6–0.79), moderate (0.4–0.59), weak (0.2–0.39), or very weak (0–0.19).

3.2 Climatological aspects of TC intensifying location from 1982 to 2017

In sub-section 3.1.4, we have briefly touched on the intensification rate as one of the suitable TC metrics to characterize TC activity in terms of intensity. Here, a significant focus has been placed on the occurrence and the movement of TC intensifying location from a latitudinal standpoint. It should be mentioned that for this analysis, the study area is delimited at 155°E on the west of the original Southwest Pacific domain, to exclude TCs that their lifetime might have been affected by landlocked nature of bordering Australian continent. The analysis was also focus on the period from 1982 to 2017 to (1) avoid any surrounding issues in relation to data quality before satellite observations and (2) match the period covered by the high resolution OISST dataset to be able to compare the observed changes of intensifying location with changes in SST.

3.2.1 Occurrence

Occurrence covers the spatial and number distribution of intensifying location over the study period. An intensifying location is defined as the latitude where the rate of change in intensity in terms of wind *V*, along the TC track is positive over a 6h period, and that particular occasion is refer to hereafter as an intensifying event. Because of the specter of rapid intensification, we have also conducted our analysis on rapidly intensifying (RI) events. TCs that underwent RI are usually associated with large forecast errors leading to a disappropriate amount of human losses and monetary costs. There is no well establish definition of RI in the existing peer-review literature for the Southwest Pacific itself, however, previous global studies (e. g., Kaplan and DeMaria 2003; Wang and Zou 2008) have provided useful information, which have

helped us to define such metric for the purpose of this study. Thus in this study, we have defined RI as an increase of at least 8 knots in 6 hours (about 32 knots $24h^{-1}$) in TC intensity.

3.2.2 Movement of intensifying location and SST changes

To examine the movement of intensifying location, we analyzed the changes in the annual averaged latitude where events have occurred. The annual averaged value is computed as a one-time averaged for all intensifying locations of all TCs in each year. To briefly justify the changed of location over the study period, SST were analyzed alongside in the sense that, it can alter the intensification process.

4. Results for TC characteristics from 1970 to 2017

The results presented in this section are based on the geographic and meteorological characteristics of TCs from 1970 to 2017 using the SPEArTC and ERSSTv5 datasets.

4.1 TC geographical distribution

The Southwest Pacific is one of the recognized birthplaces for TCs globally. Similar to other regions, TCs in the Southwest Pacific usually originate at some distance from the equator, over tropical warm waters where the necessary conditions for TC genesis are most favorable. In the Southern Hemisphere, TCs formed in a semi continuous latitudinal zone which extend from east coast of Africa to the Southwest Pacific and once formed, TCs usually follow a typically southward track. In this study, it is evident that TCs are more often than not, move in the southeasterly direction (Fig. 2). Some TCs entered the mid-latitudes and continued to travel further south, with a few going beyond 50°S (Fig. 2a) and possibly undergo extra tropical transformation. A noticeable number of TCs moved west and made landfall on the eastern Australian coast with some penetrate further inland. Some TCs, particularly the ones originated in the Gulf of Carpentaria (Fig. 1), traveled west, to the western part of Australian waters and beyond into the Southern Indian Ocean. The decadal totals for storms of all intensities (including non-TC storms) is basically decreasing (Fig. 2). The 2000–2009 decade have the smallest decadal total of tracks (105 tracks of all intensities).

The spatial distribution of TC genesis in the Southwest Pacific are predominantly in the N, NW, and W subdomains; the combined total of 358 TCs which accounts for 74.7% of the total number (Fig. 3). A total of 51 TCs were originated in the Gulf of Carpentaria and moved either east or west with limited movement neither north nor south due to dry land presence. A

notable number of TCs were also generated around the Vanuatu area and off northeastern Australia (around 150-170°E longitudinal band). The C subdomain, near Fiji, and the W subdomain, from near New Caledonia extending to the east coast of Australia (within the 15-25°S latitudinal band), had the most LV_{max} locations, which together accounted for 65.7% of the total number (Fig. 3c). As expected, LV_{max} locations tend to lie more often than not to south to southeast of the genesis locations. Four TCs been identified in the dataset (storm 14 of 1979, storm 7 of 1982, storm 7 of 1986 and storm 6 of 2003) to have only reached TC intensity during one time interval and, thus, did not have a lifetime-maximum intensity according to the definition of LV_{max} (section 3.1.2). There is relatively little TC activity in the three easternmost subdomains.

Figure 4 shows a time series of the annual average latitudes of TC genesis and V_{max}. The purpose here is to find out if there is an observed movement of the two locations during the study period. It important to mention that for this calculation, we excluded 89 TCs that formed west of 155°E in the Gulf of Carpentaria and along the northeast coast of Australia because their initiation and movements were very probably landlocked by the presence of dry land in the proximity. As it shows, the annual average TC genesis latitude (Fig. 4a) had a trend of 0.603 km yr^{-1} away from the equator, and the average V_{max} latitude (Fig. 4b) had a trend of 0.11 km yr^{-1} away from the equator and such rates are considered small. TC genesis locations had a range of 1400–2200 km from the equator, whereas V_{max} latitudes had a range of 1800–2600 km from the equator. The annual separation distance between these two average latitudes ranged from 85 and 800 km (not shown) and averaged about 370 km (not shown) over the study period.

4.2 TC number trends

Of the 479 TCs been identified, 94 (19.6%) of which were stronger TC and 385 (80.4%) remained as weaker TCs. The decadal total number of weaker TCs has declined continuously in each successive decade, however stronger TCs were relatively constant, with the exception of the first decade (1970–1979), having a total of only six stronger TCs (Table 1). An average year had about 9.98 TCs (Table 1), of which about 8.02 were weaker TCs and 2.02 were stronger TCs. In terms of the long-term variability, the annual number of TCs appears to have decreased by about 0.06 $TCyr^{-1}$ (Fig. 5a). Annual numbers of weaker TCs (Fig. 5b) also decreased by 0.104 $TCyr^{-1}$, whereas stronger TCs have shown a weakly positive trend of about 0.04 TC yr^{-1} (Fig. 5c). The year 1998 was the most active, when a total of 18 TCs occurred, of which 14 were weaker TCs and 4 were stronger, although 1997 featured 16 TCs, of which 14 were weaker TCs and 2 were stronger TCs. The quietest TC season was 2012, with three weaker TCs and only one stronger TC.

The annual number of weaker TCs tends to cover a wide range from zero to nine, in the six westernmost subdomains, whereas both the TC numbers and their variations were smaller in the three easternmost (NE, E, and SE) subdomains (Fig. 6). Long-term decreases in annual TC numbers were apparent in the NW, N, W, C, and SW subdomains, the greatest of which was −0.059 TC yr^{-1} in the W subdomain. In the NW, N, W, and C subdomains, the trends for stronger TCs appear to be positive and pronounced, the greatest of these being 0.025 stronger TC yr^{-1} in the C subdomain. Stronger TCs were absent or nearly so in the other five subdomains.

4.3 TC intensity trends

Of particular note is the marked increase in the trend of the highest annual lifetime-maximum intensity ($\hat{V}_{max}$) in the Southwest Pacific during the study period (Fig. 5d), suggesting that TCs have become more intense at an estimated rate of about 0.778 knot yr^{-1}. The highest $\hat{V}_{max}$ of 150 knots was occurred during TC Winston in 2016, and the lowest was 60 knots during TC Dora in 1971. Meanwhile, the average annual lifetime-maximum intensity ($\bar{V}_{max}$) had an upward trend of 0.266 knot yr^{-1} (Fig. 5e), which is consistent with the trend in $\hat{V}_{max}$ (Fig. 5d). There is a noticeable drop in the values of annual lifetime-maximum intensity ($\bar{V}_{max}$) around 1995-2001 (Fig. 5e), which is roughly correspond to the period with a greater number of weaker TCs (Fig. 5b). The highest annual lifetime-maximum intensification rate ($\widehat{IR}_{max}$) generally varies a little over the study period (Fig. 5f and Table 2), and the long-term trend was almost flatten (−0.001 knot h^{-1} yr^{-1}; Fig. 5f). Of a particular note was its highest $\widehat{IR}_{max}$ value of 5.933 knots h^{-1} (35.6 knots/6 h) during TC Veena in 1983. The lowest $\widehat{IR}_{max}$ value was 1.35 knots h^{-1} (8.1 knots/6 h) during TC Paula in 2001. There were 10 years (20.8%) with $\widehat{IR}_{max}$ values of <2.5 knots h^{-1} (15 knots/6 h) and 38 years (79.2%) with $\widehat{IR}_{max}$values of ≥2.5 knots h^{-1}, and in 22 years (45.8%) these $\widehat{IR}_{max}$ values occurred in the Cat 1 stage (V< 48 knots) whereas in 26 years (54.2%) they occurred at Cat 2 or higher stages (V≥ 48 knots). Some $\widehat{IR}_{max}$ calculations may be influenced by evolving observation and analysis techniques.

4.4 TC days trends

On average, every year from 1970 to 2017, had about 42.8 TC days, of which 39.24 were weaker TC days and 3.56 were stronger TC days (Table 1). The most common TCs lifetime was about 2–4 TC days, accounting for 152 (~32%) of the 475 TCs (Fig. 7). Beyond four TC days,

the frequency decreased exponentially with increasing TC lifetime. Less than 2% of the TCs had lifetimes greater than 14 TC days. The annual totals of TC days have generally decreased by about 0.352 day yr^{-1} or 3.52 days $decade^{-1}$ (Fig. 8a); while stronger TC days have increased by about 0.087 day yr^{-1} or 0.87 day $decade^{-1}$ (Fig. 8b). The largest annual number of TC days was 88.5 days in 1972 and the smallest number was 16.75 days in 2002. The largest annual number of stronger TC days was 15.5 days in 2005, and most of the years with no stronger TC days were in the 1970s, in which only 1972, 1977 and 1979 have recorded stronger TC days.

4.5 ACE trends

Although annual ACE was almost unchanged over the study period, did have a large year-to-year variability, with a slight indication of an approximately 6–8 years periodicity after 1990 (Fig. 9a). The two highest annual ACE values of ~352 × 10^3 J kg^{-1} and 353 × 10^3 J kg^{-1} have occurred during the 1992 and 1998 seasons, respectively, and a lowest of ~39 × 10^3 J kg^{-1} has occurred in 1971. A weak upward trend of 0.022 × 10^3 J kg^{-1} yr^{-1} or 0.22 10^3 J kg^{-1} $decade^{-1}$ is found, which is generally small.

On the basis of correlation analysis (Fig. 10) we examine the individual contributions from TC numbers, TC days, and TC intensity to the ACE metric. The results showed that ACE is very strongly correlated with TC days (Fig. 10c; r^2 = 0.841), strongly correlated with stronger TC days (Fig. 10d; r^2 = 0.653), moderately correlated with stronger TC number (Fig. 10b; r^2 = 0.461) and TC number (Fig. 10a, r^2 = 0.408), and weakly correlated with $\bar{V}_{max}$ (Fig. 10f; r^2 = 0.276) and $\hat{V}_{max}$ (Fig. 10e; r^2 = 0.275). These results suggest that ACE is closely linked to TC days and numbers.

4.6 PDI trends

The PDI time series also exhibits a large year-to-year variability, with a slightly upward long-term trend of 0.32×10^5 m^3 s^{-3} yr^{-1} or 3.2×10^5 m^3 s^{-3} $decade^{-1}$ (Fig. 9b). The highest annual value of ~139×10^5 m^3 s^{-3}, was observed in 1998 and the lowest, ~9×10^5 m^3 s^{-3}, was observed in 1971. A periodicity of approximately 6–8 years in the PDI time series after 1990 is more evident than it was for ACE.

Figure 11 showed that PDI is strongly correlated with strong TC days (Fig. 11d; r^2 = 0.794) and TC days (Fig. 11c; r^2 = 0.677), moderately correlated with stronger TC number (Fig. 11b; r^2 = 0.548) and $\hat{V}_{max}$ (Fig. 11e; r^2 = 0.409), and weakly correlated with $\bar{V}_{max}$ (Fig. 11f; r^2 = 0.367) and TC number (Fig. 11a; r^2 = 0.306). The results indicate that, apart from the number of TC days, PDI is largely contributed by intense TCs (stronger TC number and $\hat{V}_{max}$).

4.7 SST trends

Theoretically it is well accepted that, SST exceed 26ºC is one of the typical requirements for the cyclone genesis (Gray 1968). In this study, averages are compiled over the main TC season from October to April, over the whole domain and the subdomains. As it shows, the long-term time series of area-averaged SST (Fig. 12a) and SST anomaly (Fig. 12b) over the Southwest Pacific clearly display that SSTs have fluctuated along a stable upward trend since the mid-1970s. The SST anomaly have noticeably changed from negative to positive around 1995 and remained positive ever since. Even though not included in the main target period of this study, it should be mentioned that the late 1800s to the early 1900s were an exceptionally cool period in the Southwest Pacific. From 1917 to 2017 (Fig. 12c), the SST anomaly has increased at a rate of 0.8°C above average per 100 years (0.008°C yr^{-1}). For the study period alone (Fig. 12d),

the SST anomaly displayed a steep warming trend of 0.013°C yr^{-1}. The two most recent decades (2007–2017 and 1996–2006) are the warmest decades in the dataset. Throughout the whole study period, the year 1978 ranks as the coldest with an average SST of 25.18°C and 2017 is the warmest at 26.15°C.

The time series of the annual average SST over each of the nine subdomains are depicted in Fig. 13. It can be observed that SSTs were lower in the SW, S, and SE subdomains, with values ranging between 21°C and 22°C. In the W, C, and E subdomains, SST varied between 26°C and 28°C. The NW and N subdomains had SSTs between 28°C and 30°C, and in the NE subdomain SST varied between 26°C and 29°C. So generally, the SST in the region, varies mainly with latitude, with the warmest equatorward and coldest poleward. SST time series in all sub domains show positive trends. The strongest positive trend of 0.016°C yr^{-1} was found in the N subdomain. The NE and E subdomains both had trends of 0.015°C yr^{-1}, the C and SE subdomains had trends of 0.014°C yr^{-1}, and the NW subdomain had a trend of 0.013°C yr^{-1}. The S, SW, and W subdomains had the weakest trends of 0.011, 0.01, and 0.006°C yr^{-1}, respectively.

Figure 14 shows scatter plots of the nine TC metrics in which correlations are computed against SSTs for the Southwest Pacific from 1970 to 2017. The metric $\hat{V}_{max}$, was the most strongly correlated (Fig. 14a) against the risen SSTs (color of dots) during the study period. Even though the coefficient value was weak (r^2 = 0.294), not large enough to describe association with SST, this correlation illustrates that $\hat{V}_{max}$ may have responded to the increase in SST with time. Similarly, TC days had a very weak negative correlation with SST (r^2 = 0.119), suggesting SST's possible influence in limiting the number of TC days. Correlations between SST and other TC metrics were negligible (r^2< 0.1).

5. Results for TC intensifying location from 1982 to 2017

The results presented in this section are based on occurrence and movement of TCs intensifying location (latitudinal location) from 1982 to 2017 using the SPEArTC and OISST datasets.

5.1 Occurrence: number and spatial distribution

Table 3 tabulate the details of TCs and intensifying events that was used for this analysis. As it shows, a total of 282 TCs with 1636 intensifying events and 352 RI events were analyzed. On a decadal basis, the greatest number of 567 (34.7%) intensifying events have occurred during the 1992-2001 decade and the average per year is about 45.44 intensifying events. Moreover, the number of intensifying events per year has consistently declined after the second decade, from 56.7 during the period 1992-2001 to 29 in the period 2012-2017. In terms of RI events, the number of events has increased from 7.8 events per year during the 1992-2001 period to 12.8 events per year in the period 2012-2017. Note that, the first and the second decade have almost the same number of RI events. Clearly, it can be seen that the second part of the study period has fewer intensifying events per year (-40%) but more RI events per year (+56%). The annual number of intensifying events show a generally decreasing trend (Fig. 15a) at an estimated rate of about -1.01 events yr^{-1}, a decrease of roughly about 20% per 10 years. Large interannual variations are evident throughout, and the numbers of intensifying events per year ranging from 13 up to 107. Annual number of RI events on the other hand, has fluctuated between 1 and 26 along an increasing trend of about 0.15 events yr^{-1} (Fig. 15b), an increase of about 15% per 10 years The ratio of TC number to the number of intensifying events (Fig. 15c) exhibit a decreasing trend of about 5.7% and an increasing trend of about 3.3% for RI events (Fig. 15d).

Figure 16 show spatial distribution of the intensifying events. It seems that intensifying events are scattered over the region (except for the easternmost longitudes) and cover a wide range of latitudes extending from 5 to 35°S (Fig. 16a). The number distribution of intensifying events is shown in histograms (Figs. 16b and 16c), arranged into intervals of 5° latitude. The greatest number of about 1214 (74.2%) intensifying events have occurred within the 10-20°S band, and the highest number per 5° latitude are actually found in the 15-20°S interval which is about 659 (40.3%) events. Outside of the 10-20°S latitude band, a relatively small proportion of about 59 (3.6%) events occurred equatorward and about 363 (22.2%) events occurred poleward towards the southern limit. The climatology average intensifying latitude over 36 years is about 17.19°S (Table 3), and the average intensifying in each decade latitude ranges between 16.9°S and 17.494°S. Even though average latitude of each decade is not so far apart, the results show that there is a slightly poleward shift, particularly in the last 3 decades. The 10-20°S latitudinal band was also the most occupied in terms of RI events, which comprised of about 277 (78.7%) of the total RI events (Fig. 16c). Again, the range of average RI latitude in each decade was very small (i.e. 16.35°S -17.45°S) but slightly shift equatorward with decade. The climatology average RI location was about 16.8°S over the 36-yr period.

Figure 17 shows the distribution of intensifying events in the subdomains. It should be mentioned that, these subdomains are not the same as the subdomains in Fig. 3. It provides information about the number of intensifying events based on latitude and longitude. Even though latitudinal position was the primary aim of the analysis, it is of great important to understand the longitudinal distribution. As it shows, west of 149 W has the greatest number of intensifying events (about 1542 events of 94.3%). The eastern side of the region has only about 94 (5.7%) of the total number of intensifying events. By analysing the intensifying latitude

against the current TC intensity (Fig. 18), it can be seen that intensifying events are more frequent during the weaker TC (V <86 knots) stage. It is also shown that an almost all of intensifying events at higher latitudes are occurred during weaker TCs.

5.2 Movement of intensifying location and SST changes

Figure 19 shows the time series of annually averaged intensifying latitudes for all intensifying events (Fig. 19a) and for RI events (Fig. 19b). Intensifying location for all events fluctuates along a negative trend of about -4.1° latitude 100 yr^{-1} (Fig. 19a) from 1982 to 2017. The most equatorward annual location was about 14.786°S in 1998, and the most poleward was 23.44°S in 2009. In contrast to this poleward trend, average RI latitudes (Fig. 19b) show a positive trend of about 2.5° latitude 100yr^{-1}. Annual RI location ranged between the lower latitude of about 12.43°S in 1997 and the higher latitude of about 28.7°S in 1990.

In order to study the influence of SST on TC intensification location, we analyze the SST changes at the point of intensification (Fig. 19c) and with respect to the area and study period (Fig. 19d). At each point of intensification, the corresponding annual average SST has been increasing at rates of about 1.7 °C 100yr^{-1}. A slightly faster rate of about 5°C 100yr^{-1} was found in terms of RI events. This means that intensification is occurring at higher SSTs with time. In an attempt to examine the meridional component of SST changes, we analysed the average location of SST isotherms in each year (Fig. 20). The chosen isotherm range (25°C-29°C) was based on the sense that this is typically the range that is necessary to support TC activity, particularly genesis and intensification processes. As it shows, the location of every SST isotherm has been migrated poleward at different migration rates (Fig. 20). The migration rates

of SST isotherms ranged from -4.1° latitude $100yr^{-1}$ to -10.4° latitude yr^{-1} and higher SST isotherms migrated southward more rapidly.

6. Discussion

6.1 Overall characteristics of Tropical Cyclones

The vicinity of Vanuatu, Gulf of Carpentaria, and northeastern Australia were generally identified as the most favorable parts in the Southwest Pacific for TC genesis (Fig. 3). Very similar areas were also highlighted in previous studies to have support TC activities. For example, Diamond et al. (2013) named the area centered around Vanuatu in their study as the main TC development area for the Southwest Pacific region. Vanuatu also was included and pointed out as the main active area for TC activities by Basher and Zheng (1995), Webster et al. (2005), Kuleshov et al. (2010), and Ramsay et al. (2014). Over the Australian side of the Southwest Pacific (i.e. western part), Dare and Davidson (2004) named the Gulf of Carpentaria and the east coast of Australia as two of the three most-favored TC genesis locations. Moreover, the Vanuatu area lies roughly between the W, NW, N, and C subdomains in the present study, which contain the highest concentration of genesis locations and LV_{max} values (Fig. 3c). The W subdomain, in particular, has relatively large numbers of genesis locations and LV_{max} values.

The prevailing poleward shift of TC activity has been widely discussed globally (e.g. Daloz and Camargo 2017; Kossin et al. 2014; Sun et al. 2018, 2019). The approximately flat trend exhibited by genesis latitudes in the present study (Fig. 4a) is consistent with the findings of Terry and Gienko (2010) for the tropical South Pacific (160°E–120°W, 0°–25°S) over four

decades from the 1969–1970 to 2007–2008 season, despite their study period being shorten by a decade or so. However, the observed poleward migration trends both in terms of genesis and V_{max} latitudes in this study, which may be influenced by TC numbers, are clearly much smaller compared to those of Daloz and Camargo (2017) and Kossin et al. (2014), who linked the poleward migration to changes in environmental factors. Because there are certain to be many obvious factors that influence such analysis, identifying an adequate explanation for lack of agreement between these results remain a continuing key challenge.

Very generally, the overall number of TCs and weaker TCs are decreasing annually with some indication of a slight increase in the number of stronger TCs. (Fig. 5). It is worth mentioning that the decreasing trend of all TCs is somehow reflects total domination by weaker TCs. This overall feature of TC numbers trends in the present study is in reasonable agreement with the trends been reported by Webster et al. (2005). Once more, these findings are generally consistent with the projected number of storms and is argued to be a consequence of climate change (Emanuel 1987; Elsner et al. 2006, 2008). In contrast, Klotzbach (2006) found no significant trend over the South Pacific Ocean (5°–20°S, 155°–180°E) from 1985 to 2005, and Hoarau et al. (2017) with additional 10 year of data also found no trend in the number of strongest TCs between 1980 and 2016. In the North Atlantic basin on the other hand, Murakami et al. (2014) reported upward trends of strong TCs. The reduction in the overall number of TCs as well as the number of weaker TCs in the present study could be linked to the enhanced atmospheric stabilization process due to weaker lower troposphere warming and stronger warming aloft Maru et al. (2018). Such process can prevent further intensification, particularly to the weaker TCs which dominates the overall number of TCs in the present study. The small number of stronger TCs in the 1970s may be an effect of then-current monitoring practices. Most

WMO designated Regional Specialized Meteorological Centers and Tropical Cyclone Warning Centers who specialized in TC analysis, monitoring and forecasting have consistently used the Dvorak technique since the late 1980s (Knaff et al. 2010), so some of the TCs may be undetected and/or underestimated. However according to Terry and Gienko (2010), since stronger TCs have been in existence sufficiently long, posing a significant threat to lives and resources due to their destructive potential, it is unlikely that all TCs of such intensity gone unnoticed.

The importance of the spatial distribution of TCs across the Southwest Pacific have provided fundamental insights into analyzing trends of weaker and stronger TCs in each of the nine subdomains separately (Fig. 6). In all sub domains, the trends were generally negative; however, they were more prominent in the W, NW, N, and C subdomains. The upward trend of stronger TCs in the W, NW, N, and C subdomains is consistent with; and resembles the overall trend of stronger TCs in Southwest Pacific as a whole, which is an indication of dominance by these subdomains. Furthermore, the annual variation in the number of TCs is quite consistent with the multi-decadal count (Table 1); however, advances in detection methodologies and changes in monitoring procedures may introduce a bias toward recent decades since the newest TCs are more frequently and better sampled.

From 1970 to 2017, the annual $\hat{V}_{max}$ has trended upward in the Southwest Pacific (Fig. 5d), with an increasing rate of about 7.78 knots per decade. An increasing trend was also found by Kossin et al. (2013) for stronger TCs ($V \geq 65$ knots) but at a slightly slower rate of about 2.5 m s^{-1} per decade (4.86 knots per decade). Both findings provide powerful evidence of the increasing strength of TCs in the Southwest Pacific in terms of winds. In other regions in the world, strong TCs have also become more intense in the North Atlantic and Indian Oceans (Emanuel 2005; Elsner et al. 2008) and the northwest Pacific (Emanuel 2005; Mei and Xie

2016). TC Winston in 2016, with a V_{max} of 150 knots, is currently the most intense Southwest Pacific TC in the dataset; and with no doubt, TC Winston may be one of the strongest in the world. In addition, annual $\bar{V}_{max}$ has also increased. A noticeable drop in $\bar{V}_{max}$ values between 1996 and 2002 may be related to the dominance of weaker TCs (Cat 1–3) during these particular seasons because such metric is primarily depended on the overall identified TC number per year.

While the long-term variability of $\widehat{IR}_{max}$ has stayed approximately constant, extreme outliers are evident at irregular intervals (Fig. 5f). There is quite a number of larger $\widehat{IR}_{max}$ values (≥4 knots h^{-1} or ≥24 knots/6 h) in this study have occurred in the 1970s and the 1980s. As it shown, although most $\widehat{IR}_{max}$ values (68.75%) in this study occurred during the Cat 1 and 2 stages (Table 2), TCs of at least Cat 2 strength seem to produce larger $\widehat{IR}_{max}$ values (≥4 knots h^{-1} or ≥24 knots/6 h). Such rare events fit disastrous scenarios in which a storm intensified rapidly enough to skip an intensity category between official measurement times (typically in 6h intervals). For example, TC Prema in 1993 jumped from 60 to 90 knots (Cat 2 to Cat 4), and TC Ita in 2014 which intensified from 85 to 110 knots (Cat 3 to Cat 5). In addition the results indicate that TC intensity is likely to govern $\widehat{IR}_{max}$ and $\widehat{IR}_{max}$ is likely to occur during a TC's initial or immature stages when it is further from its V_{max} and, thus, has a greater potential to intensify faster. The dependence of intensification rate on TC intensity (in addition to SST and TC structure) is a TC characteristic that was also found by Xu and Wang (2018) over the Western North Pacific. The close association between SST and the intensification rate was also reported by Xu et al. (2016) in the North Atlantic. In this study, we found very little connection between $\widehat{IR}_{max}$ and SST (discussed shortly). Moreover, Kowch and Emanuel (2015) reported global intensification rates are controlled by randomly distributed environmental and internal processes, and Wang et al. (2015) showed that SST, heat potential, vertical wind shear, and

relative humidity are the main controlling factors over multiple decades. These studies suggest that there are likely to be many potential factors that controlled intensification rate besides the background SST, and these factors can vary across regions.

How much exposure to associated TC hazards can really contributes to the risk of being affected by a particular TC during a particular season. Depending on environmental conditions, a TC can live for a short period or much longer and generally, the longer the time spent, the higher the risk. In this study, the annual TC days, which is somewhat related to the number of TCs has decreased over the study period, while stronger TC days have increased (Fig. 8). By using the same definition of the TC day metric, Webster et al. (2005) found similar trends, not only for the Southwest Pacific but also in the North Pacific and Indian oceans. In the Western North Pacific, Kamahori et al. (2006) reported that TC days of Cat 2 or higher (based on the Saffir-Simpson scale) had been increasing over 30 years, based on both the Japan Meteorological Agency (JMA) and the JTWC dataset. However, for the case of very intense TC days (Cat 4 or higher), a contrast was found in which the JTWC dataset exhibits an increasing trend whereas the JMA dataset shows a decreasing trend.

The almost flat trend of ACE in the present study (Fig. 9a) is consistent with the trends reported by Klotzbach (2006) and Chand and Walsh (2011, 2012) despite the differences in domains. ACE inherently includes the strength and duration of all the identified TCs. By means of correlation, the contribution of TC days and stronger TC days to ACE in this study is substantial. Contributions of TC numbers and stronger TC numbers are modest and, therefore, can be interpreted as secondary contributing factors. $\hat{V}_{max}$ and $\bar{V}_{max}$ appear to have little connection with ACE. A periodicity of approximately 6–8 years has been revealed, which is in phase with the 2–8 year ENSO band (Chand and Walsh 2011), could emphasized the existence

and connectivity between ENSO and ACE. Note that TC occurrences in the South Pacific (east of 170°E) are higher in El Niño than in La Niña years (Kuleshov et al. 2008).

Although stronger TC days and TC days remained as the primary contributors to both ACE and PDI (Figs. 10 and 11), intensity metrics ($\hat{V}_{max}$ and $\bar{V}_{max}$) were generally bear more correlation with the latter (r^2 = 0.409 and 0.367, respectively) than with the former (r^2 = 0.275 and 0.276, respectively). This shows that the PDI metric is very sensitive to higher wind speeds, intensity in addition to duration in terms of TC days. In the North Atlantic and the Western North Pacific, PDI was influenced by intensity and lifetime (Emanuel, 2005). In addition, Murakami et al. (2014) found that TC genesis is the primary contributing factor to both ACE and PDI in the North Atlantic, and other metrics, such as duration and intensity, were minor.

SST is well known to have crucial impacts on regulating weather and climate variability such as TC activity on timescales of seasons and longer. The close relationship between the ocean's thermal energy and TCs' intensity in particular, has been documented in observations and model studies globally (e.g. Emanuel 2005; Webster et al. 2005; Tsuboki et al. 2015; Arora and Dash 2016). In this study the SST has been consistently warmer in the past three decades or so, than any other times in the record. These observed changes were very similar to the global changes reported by the Fifth IPCC Report (Hartmann et al. 2013) and U.S. Environmental Protection Agency (2018). This imply that SST variations in the Southwest Pacific are dominated by the global effects. We consider that averaging over the full domain, which combines the equatorial region, with the greatest amount of solar radiation, and the slightly cooler poleward regions can be seen as a possible factor that influence the average SST of the whole Southwest Pacific. Our results suggest that, while SST may have contributed somewhat to $\hat{V}_{max}$ and TC days, its contribution to other TC metrics is far less clear. The poor correlation

between SST and other TC metrics (except and $\hat{V}_{max}$ and TC days) proves that SST is not the only driving parameter that influence TC activity in the region. The aforementioned observed relationship between SST and $\hat{V}_{max}$ is supported less strongly than prior studies have found in the Northern Pacific Ocean (e.g. Kuroda et al. 1998; Wada et al. 2012); however, this could be in line with Evans' (1993) and Kotal et al. (2009)'s suggestion that SST may place an upper bound on storm intensity but is not a sufficient predictor of TC intensity. An intriguing feature is the negatively correlated SST changes with TC days which indicates that warmer SSTs may potentially reduce the number of TC days possibly through atmospheric stabilization (Sugi, 2012). It also appears that TC activities in recent decades occurred more often at warmer SSTs.

6.2 Climatology Aspects of Tropical Cyclone Intensifying Location

From this study, we can see that, on average, the Southwest Pacific is exposed to about 45.44 intensifying events per year and it is appropriate to say that, one Southwest Pacific TC can intensified at about 5.8 times on average on a 6-hr basis. These intensification periods can be consecutive or separate because some re-intensification is a characteristic of Southwest Pacific TC. Roughly speaking, these average numbers are likely to change if the existing trends were to continue, particularly with the observe declined of TC numbers which directly limit the number of intensifying events. This trend of change was also reflected on the decadal basis in terms of events per year, especially in the last 3 decades. Interestingly, the number of RI events on the other hand had increased. This means more exposure to such RI events in the present compare to the past. Surprisingly in last half of the study period (2002-2017), greater number of RI events (195 events) was recorded which is about 36% of the overall intensifying events for the same period, compared to the 14% in the first half, confirming the growing domination of RI events.

Low latitude regions generally offered typical warm tropical waters that can regulate TC activity, particularly genesis and intensification. However it is apparent that TC intensification in this study is predominantly confined to the region from 10-20°S, particularly within the 15-20°S latitudinal band if the data is arranged into 5° latitude intervals, with a climatology mean intensifying latitude of about 17.19°S. For these observations, the island and inhabitants with the aforementioned latitudinal bands are the most vulnerable in this situation. A dearth of intensifying events equatorward of 10°S, is more likely to be related to little Coriolis effect influence from the standpoint of latitude (Needham et al. 2015). Dowdy et al. (2012) reported that, the boundary for region of intensification occurs near 20°S, and slightly moves poleward (equatorward) during La Nina (El Nino) events. Climatologically, the average latitude per year for RI events is slightly equatorward in comparison to the average latitude of all events, and the same is true for decadal average latitude except the first decade. So, it is clear that RI average latitude is more often to the north of all event's average latitude. When RI latitudes are stratified into intervals of 5° latitude, almost equally number of events are found in both the 10-15°S and 15-20°S latitudinal intervals suggesting that SWP TCs tend to have the greater potential to intensify more rapidly at these latitudes. On the other hand, it is reasonable to relate the limited number of events in the eastern parts (east of 149W) of the SWP to the cooler SSTs in compassion to the central and western parts.

Despite the fact that the number of intensifying events is confined to the 10-20°S latitude band, the long-term trend shows that, the annual latitude has displaced poleward over the years. A poleward movement is also evident on a decadal basis in terms of average latitude per decade (Fig. 16, Table 3) suggesting a significant influence of interdecadal variability on long

term time series. It should be also mentioned that, because most of the intensifying events at subtropical latitudes have occurred during weaker TC period, an indication that weaker TCs may have somewhat dominate this poleward migration of intensifying location of Southwest Pacific TCs. TC intensification during weaker TC stage is a characteristic of Southwest Pacific TC as previously mentioned (in section 4.3, 6.1 and in Table 2), mainly because at this stage, TC are immature so they have greater potential to intensify further because they are far from their maximum intensities. On the other hand, RI latitudes are displaced equatorward, and with the increasing number of RI events such finding is alarming for islands and inhabitants roughly to the north of 20°S

The increase pattern of SST variability in the Southwest Pacific as explained in sub section 4.7, may have resulted in the poleward shift of the SST isotherms particularly the 25°C-29°C range. This range of SST has widely accepted to have regulate TC formation and intensification. More rapid is the poleward shift of the 28°C and 29°C isotherms but the average migration rate of isotherms overall is very similar to that of all intensifying events. This means that warmer SSTs are rapidly expanding to the poleward, and SST isotherm changes are occurring concurrently with the poleward shift in the intensifying location of all events. In this sense, the expansion of warmer SSTs poleward has important implication for the poleward migration of intensifying location, given its importance role in regulating climate and its variability. The present finding is also in agreement with the increasing evidence of the widened tropics over the past few decades (Seidel et al. 2008; Lucas et al. 2014) which led to larger warning trends in SST at higher latitudes, thus more TC activity. Moreover, since SST at the point of intensification is risen, it is stand to reason that, RI events favour the equatorward side of the Southwest Pacific because of warmer SSTs compare to higher latitudes.

7. Summary and conclusions

This study presents a comprehensive study of the characteristics of TCs in the Southwest Pacific based on the newly developed SPEArTC best-track along with the ERSSTv5 and OISST dataset. Careful consideration has been given to the quality of the data and particularly the evolving monitoring technologies and operational practices. Therefore, the findings of this study rely heavily on the accuracy of the datasets, specifically the SPEArTC in capturing TC activity.

7.1 Characteristics of TCs from 1970 to 2017

In the first part of this study, our choice of a larger study domain than previous studies may be an advantage over prior attempts as it includes more TCs. The study employed a diverse variety of TC metrics and linked them to the gradual rise in SST. The main primary findings are:

- The W, NW, N, and C subdomains, typically west of Fiji, are identified to be the most favorable locations for TC activity in the Southwest Pacific; thus, the risks and vulnerability of populations are highly elevated across these regions.
- The location where TCs originated (TC genesis) and where they reached their lifetime maximum intensity (V_{max}) remained almost unchanged during the past decades from 1970 to 2017, which suggests little shift in the dominant areas affected by TCs.
- Although the year-to-year fluctuation in the number of TCs in the Southwest Pacific is quite large, with a range of 4–18, we found a 48-year average of around 10 TCs (of which two were stronger TCs) per TC season. The overall number of TCs appears to have decreased. The number of stronger TCs have slightly

increased but it is highly likely an artifact, possibly due to data uncertainties in the 1970s, which is consistent with Hoarau et al. (2017)'s study, which found no trends in the number of strongest TCs over the 1980–2016 period. However, the strength of stronger TCs have increased noticeably which is displayed by upward trend in $\hat{V}_{max}$ and $\bar{V}_{max}$. Such high-impact events include TC Pam in 2015 with V_{max} = 135 knots and TC Winston in 2016 with V_{max} = 150 knots.

- Maximum intensification (IR_{max}) occurred at all TC stages (Cat 1 to Cat 5), but most (68.75%) occurred during the Cat 1 and 2 stages. This indicates that weaker TCs may intensify faster because they are further from their peak intensity. However, larger IR_{max} values (≥4 knots h^{-1} or ≥24 knots/6 h) are likely to occur during TCs of at least Cat 2 strength, which suggests faster intensification rates may be somewhat related to the current TC stage. Because the highest IR_{max} value in each year ($\widehat{IR}_{max}$) has no long-term trend, the occurrence of intensifying TCs with higher intensification rates is likely to continue.
- There are about 42.8 TC days (of which 3.56 were stronger TC days) per TC season in the Southwest Pacific. The most frequent TC length is 2 to 4 days. The total TC days ($V \geq 34$ knots) has decreased while stronger TCs ($V \geq 86$ knots) live longer.
- There are no apparent trends in ACE and PDI over the study period. The results also suggest both quantities are controlled mainly by TC days and secondarily by TC number and intensity; however, $\hat{V}_{max}$ and stronger TC numbers tend to contribute more strongly to PDI than to ACE.

- The averaged SST exhibited a gradual warming trend of about 0.624°C over the past 48 years; however, this trend is only weakly correlated with TC activity. This finding suggests that, while SST may contribute to the uppermost TC intensity and fewer TC days, it does not appear to be the dominant environmental determinant of TC activity, nor does warmer SST alone necessarily explain TC activity trends.

Our findings are somewhat consistent with theoretical expectations of the change in TC activity under climate change, particularly in TC overall frequency and $\hat{V}_{max}$ intensity. However, the small trends found in genesis latitude, V_{max} latitude, $\widehat{IR}_{max}$, ACE, and PDI tell us that TC activity has not changed much, suggesting that the Southwest Pacific region is likely to remain most vulnerable to such TC impacts at irregular interannual periods.

7.2 Climatological aspects of TC Intensifying Latitude from 1982 to 2017

The second part of the study highlighted some important points concerning tropical cyclone intensifying latitudes in the region enclosed by 5-35°S, 155E-120W, over 36-yr period from 1982 to 2017. These results show that:

- There is some evidence that the number of intensifying events have decreased considerably, which is be related to the declined in the overall number of TCs in the region however the ratio of rapidly intensifying counterpart have increased.

- Intensification occurs most frequently in the confines of the latitude bands 10°-20°S, however, in intervals of 5° latitude, the 15-20°S band has the highest concentration.
- The latitude where tropical cyclone intensification exhibits a clear poleward movement (all events) with a slightly equatorward migration in terms of rapidly intensifying latitude. This migration poleward is more likely to be influenced by the poleward warming of SSTs in the region.

Finally, the higher concentrations of intensifying activity in the 10-20°S latitude band, indicates that the nations and territories within the vicinity are apparently more vulnerable to such intensifying events. However, it should be mentioned that the observed poleward (equatorward) displacements of all intensifying events (RI events), suggest that, heightened risks further to the south (north) can be expected in the near-future, and would potentially have profound impacts if the current trends were to continue.

7.3 Way Forward

The present study also urges the necessity of a more thorough investigation of other factors apart from SST that may have responsible for the observed variations of TC activity in the Southwest Pacific. Future work looks toward exploring other climatological drivers of TC activity through more research, to unravel more and better characterize specific behavior of TCs on various timescales.

Acknowledgments

First of all, I am indebted to my humble and most intelligent supervisor Prof. Kazuhisa Tsuboki for his technical guidance, encouraging association and patience throughout the period of my research work in Nagoya University. Without you, I would not have the courage to strive and complete this effort. Thank you so much for being responsive and supportive.

I am also thankful to Prof. Shinoda, Prof. Murakami, Dr. Kanada, Dr. Yoshioka and every member of the Meteorology Laboratory for providing a friendly, lively and congenial working atmosphere. I wish to thank Mr. Masaya Kato for all the kind assistance provided whenever I needed, I have been particularly lucky to be roomed together. A special thank particularly to Ms. Mariko Kayaba for the polite and ready assistance. The support I received from these individuals is something that will be very difficult to give back. Thank you for hosting me throughout my study.

To my friends and family, thank you for your advice, support and encouragement that keep me going along the way in spite of being far away from me. I hope this piece of work will remind you of the reason why I was away from you during some of the most important days of our lives.

I would like to express my gratitude to the Japanese Government Monbugakusho Scholarship (MEXT), for providing the financial support to fund my study in Japan. I also wish to take this opportunity to thank the JSPS KAKENHI Grant Number JP16H06311 for the financial support for my two (2) journal papers (1 published, 1 submitted) that constitute the main body of this thesis.

Above all, Glory and Honor be to the Almighty God

References

Arora, K., and P. Dash, 2016: Towards dependence of tropical cyclone intensity on sea surface temperature and its response in a warming world. *Climate*, **4**, 30.

Barnett, J., 2001: Adapting to climate change in Pacific Island countries: The problem of uncertainty. *World Development*, **29**, 977-993.

Basher, R. E., and X. Zheng, 1995: Tropical cyclones in the southwest Pacific: Spatial patterns and relationships to Southern Oscillation and sea surface temperature. *J. Climate*, **8**, 1249–1260.

Bell, G. D., M. S, Halpert, R. C. Schnell, R.W. Higgins, J. Lawrimore, V. E. Kousky, R. Tinker, W. Thiaw, M. Chelliah. and A. Artusa, 2000: Climate Assessment for 1999. *Bull. Amer. Meteor. Soc*., **81**, Si–S50.

Blunden, J., and D. S. Arndt, 2016: State of the climate in 2015. *Bull. Amer. Meteor. Soc.*, **97**, Si–S275.

Blunden, J., and D. S. Arndt, 2017: State of the climate in 2016. *Bull. Amer. Meteor. Soc.*, **98**, Si–S277.

Callaghan, J., and S. B. Power, 2011: Variability and decline in the number of severe tropical cyclones making land-fall over eastern Australia since the late nineteenth century. *Climate Dyn*., **37**, 647–662.

Camargo, S. J., and A. H. Sobel, 2005: Western North Pacific tropical cyclone intensity and ENSO. *J. Climate*, **18**, 2996–3006.

Chand, S., and K. Walsh, 2009: Tropical Cyclone Activity in the Fiji Region: Spatial Patterns and Relationship to Large-Scale Circulation. *J. Climate*, **22**, 3877–3893.

Chand, S. S., and K. J. Walsh, 2011: Influence of ENSO on tropical cyclone intensity in the Fiji region. *J. Climate*, **24**, 4096–4108.

Chand, S. S., and K. J. Walsh, 2012: Modeling seasonal tropical cyclone activity in the Fiji Region as a binary classification problem. *J. Climate*, **25**, 5057–5071.

Chu, J.-H., C. R. Sampson, A. S. Levine, and E. Fukada, 2002: The Joint Typhoon Warning Center tropical cyclone best-tracks, 1945-2000. *U.S. Naval Research Laboratory Rep*. *NRL/MR/ 7540-02-16*, **22** pp.

Corporal-Lodangco, I. L., L. M. Leslie, and P. J. Lamb, 2016: Impacts of ENSO on Philippine tropical cyclone activity. *J. Climate*, **29**, 1877–1897.

Daloz, A. S., and S. J. Camargo, 2017: Is the poleward migration of tropical cyclone maximum intensity associated with a poleward migration of tropical cyclone genesis?. *Climate Dyn.*, **50**, 705–715.

Dare, R. A., and N. E. Davidson, 2004: Characteristics of tropical cyclones in the Australian region. *Mon. Wea. Rev.*, **132**, 3049–3065.

Diamond, H. J., A. M. Lorrey, K. R. Knapp, and D. H. Levinson, 2012: Development of an enhanced tropical cyclone tracks database for the southwest Pacific from 1840 to 2010. *Int. J. Climatol*., **32**, 2240–2250.

Diamond, H. J., A. M. Lorrey, and J. A. Renwick, 2013: A southwest Pacific tropical cyclone climatology and linkages to the El Niño–Southern Oscillation. *J. Climate*, **26**, 3–25.

De Scally, F. A., 2008: Historical tropical cyclone activity and impacts in the Cook Islands, *Pac. Sci*., **62**, 443–459

Dowdy, A. J., L. Qi, D. Jones, H. Ramsay, R. Fawcett, and Y. Kuleshov, 2012: Tropical cyclone climatology of the South Pacific Ocean and its relationship to El Niño–Southern Oscillation. *J. Climate*, **25**, 6108–6122.

Dvorak, V. F., 1972: A technique for the analysis and forecasting of tropical cyclone intensities from satellite pictures. NOAA Tech. Rep. NESS 36, 15 pp.

Dvorak, V. F., 1975: Tropical cyclone intensity analysis and forecasting from satellite imagery. *Mon. Wea. Rev.*, **103**, 420–430.

Dvorak, V. F., 1984: Tropical cyclone intensity analysis using satellite data. NOAA Tech. Rep. NESDIS 11, 47 pp.

Elsner, J., A. Tsonis, and T. Jagger, 2006: High-Frequency Variability in Hurricane Power Dissipation and Its Relationship to Global Temperature. *Bull. Amer. Meteor. Soc.*, **87**, 763–768.

Elsner, J. B., J. P. Kossin, and T. H. Jagger, 2008: The increasing intensity of the strongest tropical cyclones. *Nature*, **455**, 92-95.

Emanuel, K. A., 1987: The dependence of hurricane intensity on climate. *Nature*, **326**, 483–485.

Emanuel, K., 2005: Increasing destructiveness of tropical cyclones over the past 30 years. *Nature*, **436**, 686–688.

Emanuel, K., 2007: Environmental factors affecting tropical cyclone power dissipation. *J. Climate*, **20**, 5497–5509.

Evans, J. L., 1993: Sensitivity of tropical cyclone intensity to sea surface temperature. *J. Climate*, **6**, 1133–1140.

Frank, W. M., and G. S. Young, 2007: The interannual variability of tropical cyclones. *Mon. Wea. Rev.*, **135**, 3587–3598.

Ginger, J., D. Henderson, C. Leitch, and G. Boughton, 2007: Tropical Cyclone Larry: Estimation of wind field and assessment of building damage. *Aust. J. Struct. Eng*., **7(3)**, 209–224.

Goebbert, K. H., and L. M. Leslie, 2010: Interannual variability of northwest Australian tropical cyclones. *J. Climate*, **23**, 4538–4555.

Government of Vanuatu, 2015: Post-Disaster need assessment: *Tropical Cyclone Pam, March 2015*. [Available at https://cop23.com.fj/wp-content/uploads/2017/06/vanuatu_pdna_cyclone_pam_2015.pdf.]

Government of Fiji, 2016: Post-Disaster need assessment: *Tropical Cyclone Winston, February 20, 2016*. [Available at https://www.gfdrr.org/sites/default/files/publication/Post%20Disaster%20Needs%20Assessments%20CYCLONE%20WINSTON%20Fiji%202016%20(Online%20Version).pdf]

Government of Tonga, 2018: Tonga: *Post Disaster Rapid Assessment: Tropical Cyclone Gita, February 12, 2018*. [Available at: https://www.gfdrr.org/sites/default/files/publication/tonga-pdna-tc-gita-2018.pdf]

Gray, W. M., 1968: Global view of the origin of tropical disturbances and storms. *Mon. Wea. Rev.*, **96**, 669–700.

Gray, W. M., 1977: Tropical cyclone genesis in the western North Pacific. *J. Meteorol. Soc*., Japan, 55, 465–482.

Gualdi, S., E. Scoccimarro, and A. Navarra, 2008: Changes in tropical cyclone activity due to global warming: Results from a high-resolution coupled general circulation model. *J. Climate*, **21**, 5204–5228.

Guard, C., and M. A. Lander, 1999: A scale relating tropical cyclone wind speed to potential damage for the tropical Pacific Ocean region: a user's manual. WERI Technical Report 86.

Haig, J., J. Nott, and G. J. Reichart, 2014: Australian tropical cyclone activity lower than at any time over the past 550– 1,500 years. *Nature*, **505**, 667–671.

Hartmann, D. L., A. M. G. Klein Tank, M. Rusticucci, L. V. Alexander, S. Brönnimann, Y. Charabi, F. J. Dentener, E. J. Dlugokencky, D. R. Easterling, A. Kaplan, B. J. Soden, P. W. Thorne, M. Wild, and P. M. Zhai, 2013: Observations: Atmosphere and Surface. In: *Climate Change 2013: The Physical Science Basis. Contribution of Working Group I to the Fifth Assessment Report of the Intergovernmental Panel on Climate Change* [Stocker, T.F., D. Qin, G. K. Plattner, M. Tignor, S. K. Allen, J. Boschung, A. Nauels, Y. Xia, V. Bex and P. M. Midgley (eds.)]. Cambridge University Press, Cambridge, United Kingdom and New York, NY, USA, 159–254.

Hassim, M. E., and K. J. Walsh, 2008: Tropical cyclone trends in the Australian region. *Geochem. Geophys. Geosyst*., **9,** Q07v07, DOI:10.1029/2007GC001804.

Hoarau, K., L. Chalonge, F. Pirard, and D. Peyrusaubes, 2018: Extreme tropical cyclone activities in the southern Pacific Ocean. *Int. J. Climatol.*, **38**, 1409–1420.

Holland, G., 1981: On the quality of the Australian tropical cyclone data base, *Aust. Met. Mag.*, **29**, 169–181.

Huang, B., P. Thorne, V. Banzon, T. Boyer, G. Chepurin, J. Lawrimore, M. Menne, T. Smith, R. Vose, and H. Zhang, 2017: Extended Reconstructed Sea Surface Temperature, Version 5 (ERSSTv5): Upgrades, Validations, and Intercomparisons. *J. Climate*, **30**, 8179–8205.

Iizuka, S., and T. Matsuura, 2012: Analysis of tropical cyclone activity in the southern hemisphere using observation and CGCM simulation. *Cyclones: Formation, Triggers, and Control*. Oouchi, K., and H. Fudeyasu (eds.), Nova Science Publishers, 37–35.

IPCC Secretariat, 2013: IPCC Factsheet: What is IPCC? https://www.ipcc.ch/site/assets/uploads/2018/02/FS_what_ipcc.pdf

Kamahori, H., N. Yamazaki, N. Mannoji, and K. Takahashi, 2006: Variability in intense tropical cyclone days in the western North Pacific. *SOLA*, **2**, 104–107.

Kaplan, J., and M. DeMaria, 2003: Large-scale characteristics of rapidly intensifying tropical cyclones in the North Atlantic basin. *Wea. Forecasting*, **18**, 1093–1108.

Klotzbach, P. J., 2006: Trends in global tropical cyclone activity over the past twenty years (1986-2005). *Geophys. Res. Lett.*, **33**, L10805, DOI:10.1029/2006GL025881.

Klotzbach, P. J., and C. W. Landsea, 2015: Extremely intense hurricanes: Revisiting Webster et al. (2005) after 10 years. *J. Climate*, **28**, 7621–7629.

Knaff, J. A., D. P. Brown, J. Courtney, G. M. Gallina, and J. L. Beven, 2010: An evaluation of Dvorak technique–based tropical cyclone intensity estimates. *Wea. Forecasting*, **25**, 1362–1379.

Knaff, J. A., and R. M. Zehr, 2007: Reexamination of tropical cyclone wind–pressure relationships. *Wea. Forecasting*, **22**, 71–88.

Knapp, K. R., M. C. Kruk, D. H. Levinson, H. J. Diamond, and C. J. Neuman, 2010: The International Best Track Archive for Climate Stewardship (IBTrACS). *Bull. Amer. Meteor. Soc.*, **91**, 363–376.

Knutson, T. R., and R. E. Tuleya, 2008: Tropical cyclones and climate change: revisiting recent studies at GFDL. In: Diaz HF, Murnane RJ (eds) Climate extremes and society. Cambridge University Press, Cambridge, p 120–143

Kossin, J. P., T. L. Olander, and K. R. Knapp, 2013: Trend analysis with a new global record of tropical cyclone intensity. *J. Climate*, **26**, 9960–9976.

Kossin, J. P., K. A. Emanuel, and G. A. Vecchi, 2014: The poleward migration of the location of tropical cyclone maximum intensity. *Nature*, **509**, 349–352.

Kotal, S. D., P. K. Kundu, and S. K. Roy Bhowmik, 2009: An analysis of sea surface temperature and maximum potential intensity of tropical cyclones over the Bay of Bengal between 1981 and 2000. *Meteorol. Appl.*, **16**, 169–177.

Kowch, R., and K. Emanuel, 2015: Are special processes at work in the rapid intensification of tropical cyclones?. *Mon. Wea. Rev.*, **143**, 878–882.

Kruk, M. C., K. R. Knapp, and D. H. Levinson, 2010: A technique for combining global tropical cyclone best track data. J. Atmos. Oceanic Technol., 27, 680–692.

Kuleshov, Y., L. Qi, R. Fawcett, and D. Jones, 2008: On tropical cyclone activity in the Southern Hemisphere: Trends and the ENSO teleconnection. *Geophys. Res. Lett.*, **35**, L14S08, DOI:10.1029/2007GL032983.

Kuleshov, Y., R. Fawcett, L. Qi, B. Trewin, D. Jones, J. McBride, and H. Ramsay, 2010: Trends in tropical cyclones in the South Indian Ocean and the South Pacific Ocean. *J. Geophys. Res.*, **115**, D01101, DOI:10.1029/2009JD012372

Kuroda, M., A. Harada, and K. Tomine, 1998: Some aspects on sensitivity of typhoon intensity to sea surface temperature. *J. Meteor. Soc. Japan*, **76**, 145–151.

Landsea, C. W., B. A. Harper, K. Hoarau, and J. A. Knaff, 2006: Can we detect trends in extreme tropical cyclones? *Science*, **313**, 452–454.

Li, R. C., W. Zhou, C. M. Shun, and T. C. Lee, 2017: Change in destructiveness of landfalling tropical cyclones over China in recent decades. *J. Climate*, **30**, 3367–3379.

Lucas, C., B. Timbal, and H. Nguyen, 2014: The expanding tropics: A critical assessment of the observational and modeling studies. *Wiley Interdiscip. Rev.: Climate Change*, **5**, 89–112.

Magee, A. D., D. C. Verdon-Kidd, and A. S. Kiem, 2016: An intercomparison of tropical cyclone best-track products for the southwest Pacific. *Nat. Hazards Earth Syst. Sci.*, **16**, 1431–1447.

Magee, A. D., and D. C. Verdon-Kidd, 2018: On the relationship between Indian Ocean sea surface temperature variability and tropical cyclogenesis in the southwest Pacific. *Int. J Climatol*., **38**, e774–e795, https://doi.org/10.1002/joc.5406.

Magee, A.D., and D. C. Verdon-Kidd, 2019: Historical Variability of southwest Pacific tropical cyclone counts since 1855. *Geophys. Res. Lett*., **46**, 6936–6945.

Maru, E., T. Shibata, and K. Ito, 2018: Statistical analysis of tropical cyclones in the Solomon islands. *Atmosphere*, **9**, 227.

Mei, W., and S. P. Xie, 2016: Intensification of landfalling typhoons over the northwest Pacific since the late 1970s. *Nat. Geosci.*, **9**, 753–757.

Murakami, H., and M. Sugi, 2010: Effect of model resolution on tropical cyclone climate projections. *SOLA*, **6**, 73–76.

Murakami, H., T. Li, and P. C. Hsu, 2014: Contributing factors to the recent high level of accumulated cyclone energy (ACE) and power dissipation index (PDI) in the North Atlantic. *J. Climate*, **27**, 3023–3034.

Needham, H. F., B. D. Keim, and D. Sathiaraj, 2015: A review of tropical cyclone-generated storm surges: Global data sources, observations, and impacts. *Rev. Geophys*., **53**, 545–591

Nicholls. N., C. Landsea, and J. Gill, 1998: Recent trends in Australian regional tropical cyclone activity. *Meteor Atmos. Phys*., **65**, 197-205.

Oouchi, K., J. Yoshimura, H. Yoshimura, R. Mizuta, S. Kusunoki, and A. Noda, 2006: Tropical cyclone climatology in a global-warming climate as simulated in a 20km-mesh global atmospheric model: Frequency and wind intensity analysis. *J. Meteor. Soc. Japan*, **84**, 259−276.

Pielke, R. A., J. Gratz, C. W. Landsea, D. Collins, M. A. Saunders, and R. Musulin, 2008: Normalized hurricane damages in the United States: 1900–2005. *Nat. Hazards Rev*., **9**, 29–42.

Ramsay, H. A., M. B. Richman, and L. M. Leslie, 2014: Seasonal tropical cyclone predictions using optimized combinations of ENSO regions: Application to the Coral Sea basin. *J. Climate*, **27**, 8527–8542.

Rappaport, E. N., J. L. Franklin, L. A. Avila, S. R. Baig, J. L. Beven, E. S. Blake, C. A. Burr, J. G.Jiing, C. A. Juckins, R. D. Knabb, C. W. Landsea, M. Mainelli, M. Mayfield, C. J. McAdie, R. J. Pasch, C. Sisko, S. R. Stewart, and A. N. Tribble, 2009: Advances and challenges at the National Hurricane Center. *Wea. Forecasting*, **24**, 395–419.

Reynolds, R. W., T. M. Smith, C. Liu, D. B. Chelton, K. S. Casey, and M. G. Schlax, 2007: Daily high-resolution-blended analyses for sea surface temperature. *J. Climate*, **20**, 5473–5496.

Seidel, D. J., Q. Fu, W. Randel, and T. Reichler, 2008: Widening of the tropical belt in a changing climate. *Nat. Geosci*., **1**, 21–24.

Stewart, M. G., 2003: Cyclone damage and temporal changes to building vulnerability and economic risks for residential construction. *J. Wind Eng. Ind. Aerodyn*., **91(5)**, 671–691.

Sugi, M., 2012: Reduction of Global Tropical Cyclone Frequency Due to Global Warming. In Cyclones: Formation, Triggers, and Control. *Nova Science Publishers*, 115–123 pp.

Sun, Y., T. Li, Z. Zhong, L. Yi, X. Chen, Y. Ha, J. Zhu, Y. Shen, Z. Xu, and Y. Hu, 2018: A recent reversal in the poleward shift of western North Pacific tropical cyclones. *Geophys. Res. Lett*., **45**, 9944–9952.

Sun, J., D. Wang, X. Hu, Z. Ling, and L. Wang, 2019: Ongoing poleward migration of tropical cyclone occurrence over the western North Pacific Ocean. *Geophys. Res. Lett.*, **46**, 9110–9117.

Terry, J. P., and G. Gienko, 2010: Climatological aspects of South Pacific tropical cyclones, based on analysis of the RSMC-Nadi (Fiji) regional archive. *Clim. Res.*, **42**, 223–233.

Trewin, B., 2008: An enhanced tropical cyclone data set for the Australian region. Preprints, *20th Conf. on Climate Variability and Change*, New Orleans, LA, Amer. Meteor. Soc., JP3.1. [Available online at http://ams.confex.com/ams/88Annual/techprogram/paper_128054.htm.]

Tsuboki, K., M. K. Yoshioka, T. Shinoda, M. Kato, S. Kanada, and A. Kitoh, 2015: Future increase of supertyphoon intensity associated with climate change. *Geophys. Res. Lett.,* **42**, 646–652.

U.S. Environmental Protection Agency, 2018: Climate change indicators in the United States, 2016, fourth edition. [Available at https://www.epa.gov/climate-indicators/downloads-indicators-report]

Velden, C. S., T. L. Olander, and R. M. Zehr, 1998: Development of an objective scheme to estimate tropical cyclone intensity from digital geostationary satellite infrared imagery. *Wea. Forecasting*, **13**, 172–186.

Villarini, G., and G. A. Vecchi, 2013: Multiseason lead forecast of the North Atlantic power dissipation index (PDI) and accumulated cyclone energy (ACE). *J. Climate*, **26**, 3631–3643.

Vincent, E. M., M. Lengaigne, C. E. Menkes, N. C. Jourrdain, P. Marchesiello, and G. Madec, 2009: Interannual variability of the South Pacific convergence zone and implication for tropical cyclone genesis. *Clim. Dyn*., **36**, 1881–1896.

Wada, A., N. Usui, and K. Sato, 2012: Relationship of maximum tropical cyclone intensity to sea surface temperature and tropical cyclone heat potential in the North Pacific Ocean. *J. Geophys. Res.,* **117**, D11118, DOI:10.1029/2012JD017583

Wang, X., C. Wang, L. Zhang, and X. Wang, 2015: Multidecadal variability of tropical cyclone rapid intensification in the Western North Pacific. *J. Climate*, **28**, 3806–3820.

Wang, B., and X. Zhou, 2008: Climate variability and predictability of rapid intensification in tropical cyclones in the western North Pacific. *Meteor. Atmos. Phys*., **99**, 1–16.

Webster, P. J., G. J. Holland, J. A. Curry, and H.R. Chang, 2005: Changes in tropical cyclone number, duration, and intensity in a warming environment, *Science*, **309**, 1844–1846.

World Bank. 2006: Not if, but when: adapting to natural hazards in the Pacific Island region. A Policy Note, The World Bank, East Asia and the Pacific Region, Pacific Islands Country Management Unit, Washington, DC.

World Bank, 2013: *Acting on climate change and disaster risk for the Pacific*. 16 pp.

World Meteorological Organization, 2016: Tropical Cyclone Operational Plan for the South Pacific and South-East Indian Ocean. [Available at https://www.wmo.int/pages/prog/www/tcp/documents/RAV_OpPlan_TCP-24_WMO-1181_2016_Final.pdf]

World Meteorological Organization, 2017: Global guide to tropical cyclone forecasting. 399pp. [Available at https://cyclone.wmo.int/pdf/Global-Guide-to-Tropical-Cyclone-Forecasting.pdf]

Xu, J., Y. Wang, and Z. M. Tan, 2016: The relationship between sea surface temperature and maximum intensification rate of tropical cyclones in the North Atlantic. *J. Atmos. Sci.*, **73**, 4979–4988.

Xu, J., and Y. Wang, 2018: Dependence of tropical cyclone intensification rate on sea surface temperature, storm intensity, and size in the western North Pacific. *Wea. Forecasting*, **33**, 523–537.

Zhang, W., G. A. Vecchi, H. Murakami, T. L. Delworth, K. Paffendorf, L. Jia, G. Villarini, R. Gudgel, F. Zeng, and X. Yang, 2016: Influences of natural variability and Anthropogenic forcing on the extreme 2015 accumulated cyclone energy in the western North Pacific. *Bull. Amer. Meteor. Society.*, **97**, S131–S135.

Figures

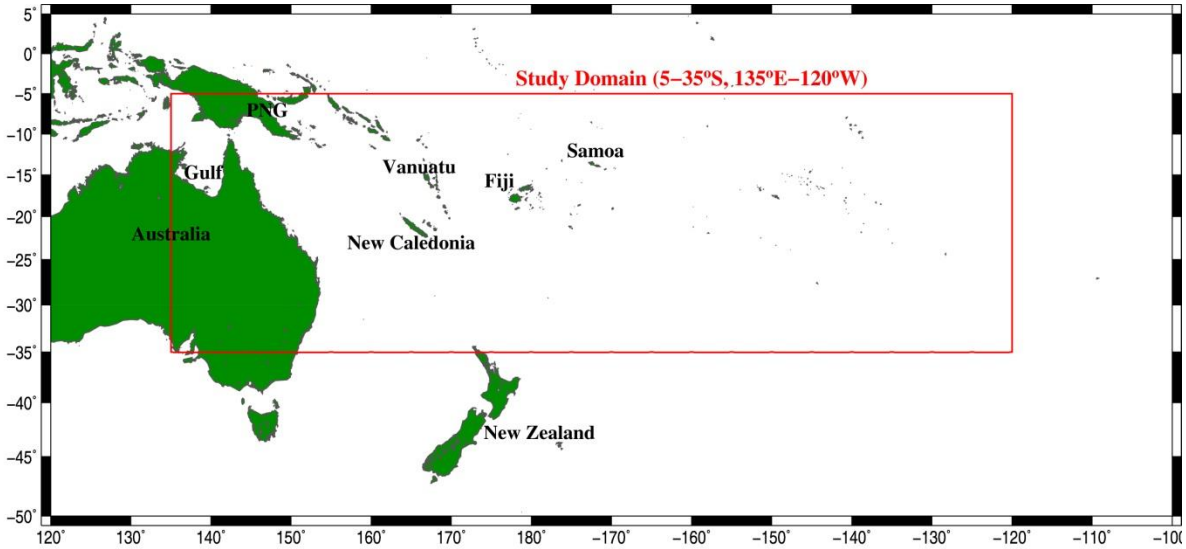

Fig. 1. Map of the Southwest Pacific showing the domain of the of the first part of the present study (Study Domain, red outline).

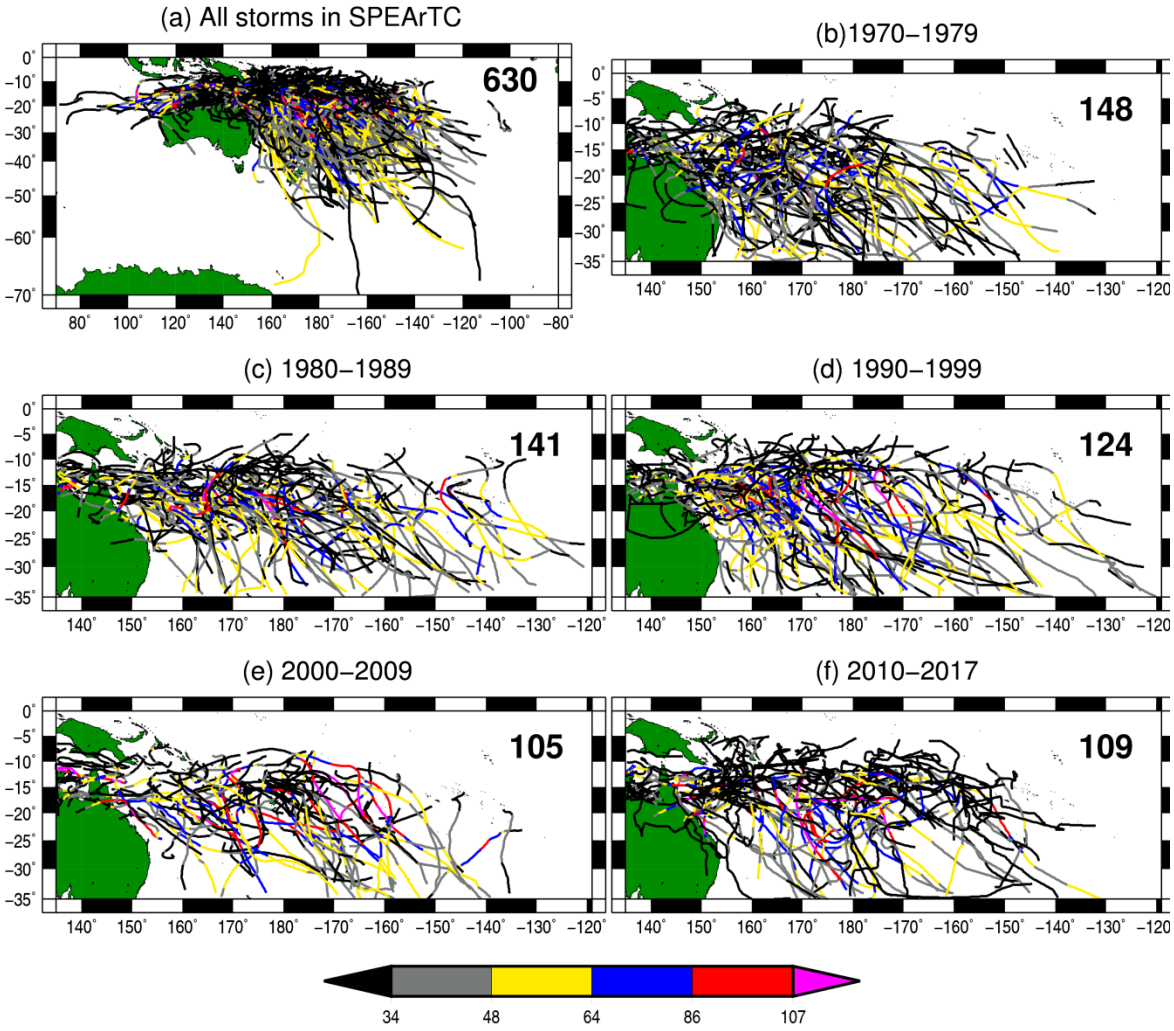

Fig. 2. TC Track distributions of (a) all storms in the SPEArTC dataset, (b) 1970–1979 storms, (c) 1980–1989 storms, (d) 1990–1999 storms, (e) 2000–2009 storms, and (f) 2010–2017 storms. The colors represent storm categories (Cat) based on wind levels from non-TC storms (0–34 knots, black), Cat 1 ($34 \leq V < 48$ knots, gray), Cat 2 ($38 \leq V < 64$ knots, yellow), Cat 3 ($64 \leq V \leq 86$ knots, blue), Cat 4 ($86 \leq V \leq 107$ knots, red), and Cat 5 ($V \geq 107$ knots, magenta). Storms are categorized according to the WMO/Australia scale. The number indicates the number of tracks.

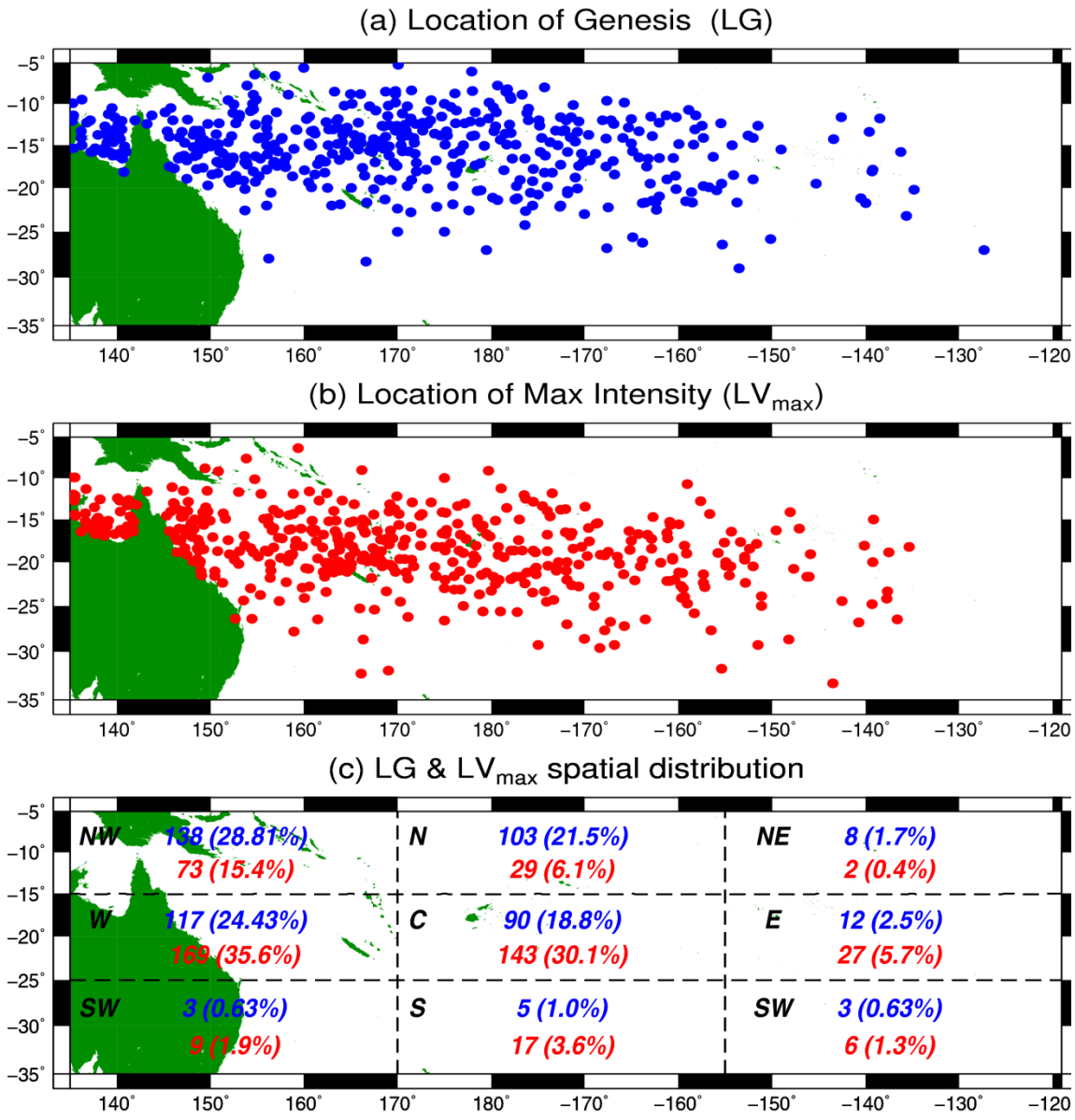

Fig. 3. (a) Geographical distribution of TC genesis points (LGs; blue), (b) locations where lifetime-maximum TC intensity is reached (LV_{max}; red), and (c) number and percentage (in brackets) of LGs (blue letters) and LV_{max} (red letters) in the subdomains of the study domain.

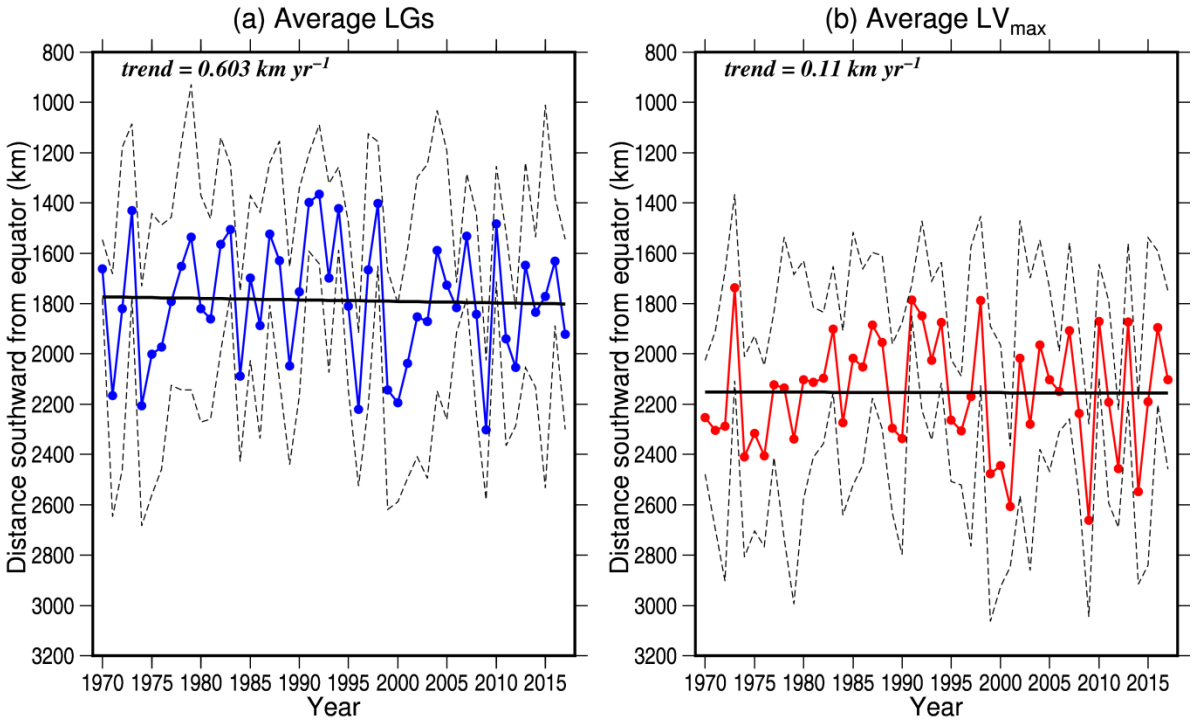

Fig. 4. Time series of the annual average locations of (a) genesis (LGs) and (b) lifetime-maximum intensity (LV_{max}) of TCs in the Southwest Pacific. The distance is south of the Equator. The dotted lines represent standard deviations corresponding to the mean values; the black line represents the linear trend. The numbers (trend) represent the slope (km yr^{-1}).

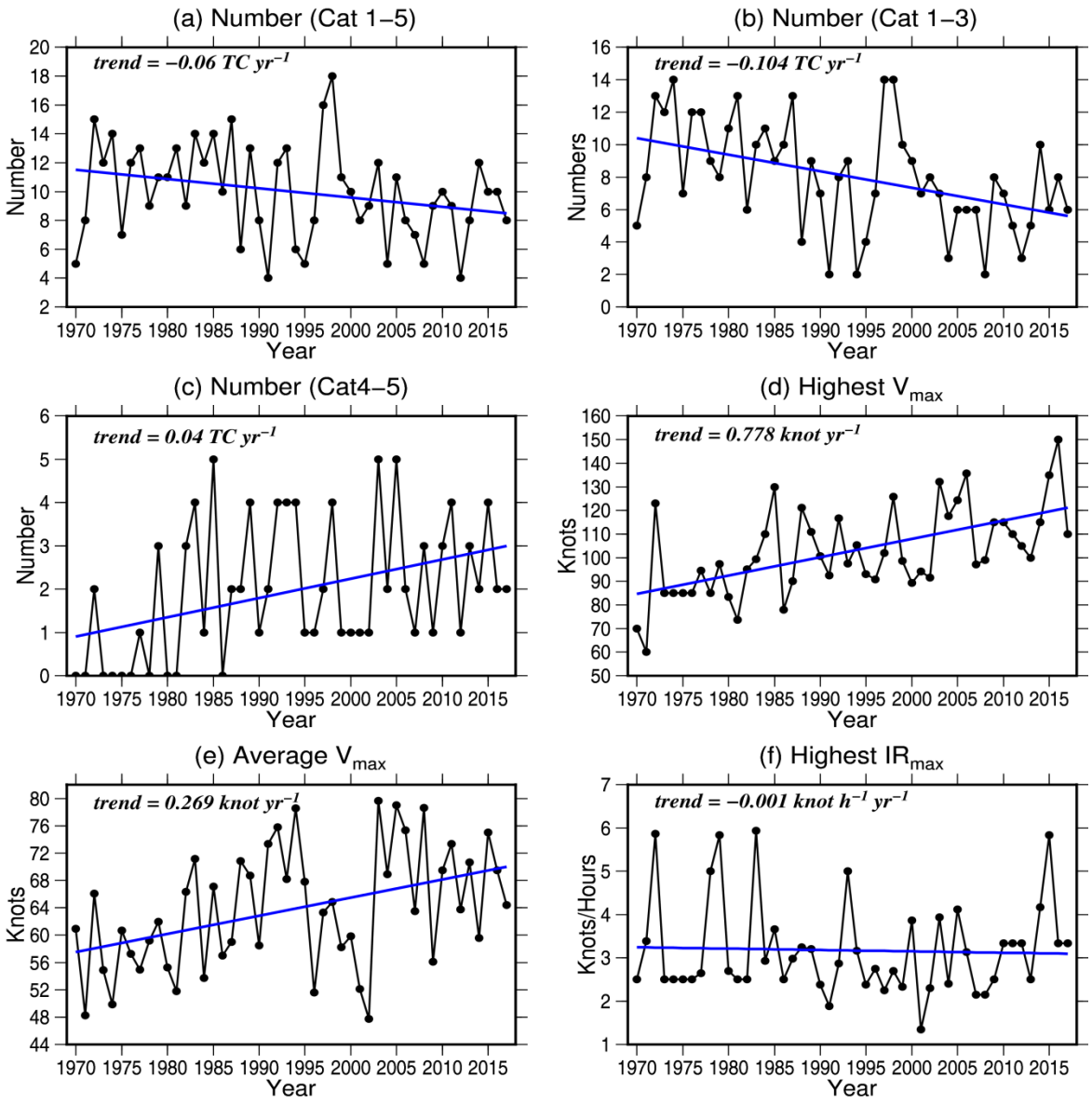

Fig. 5. Interannual variation in various metrics for TC activity during 1970–2017. (a) Number of TCs, (b) number of weaker TCs (Cat 1–3), (c) number of stronger TCs (Cat 4–5), (d) highest annual lifetime-maximum TC intensity ($\hat{V}_{max}$; knots), (e) average annual lifetime-maximum intensity ($\bar{V}_{max}$; knots), and (f) highest annual lifetime-maximum intensification rate ($\widehat{IR}_{max}$; knots h^{-1}). The blue line shows the linear trend, and the number in the top left corner is its slope.

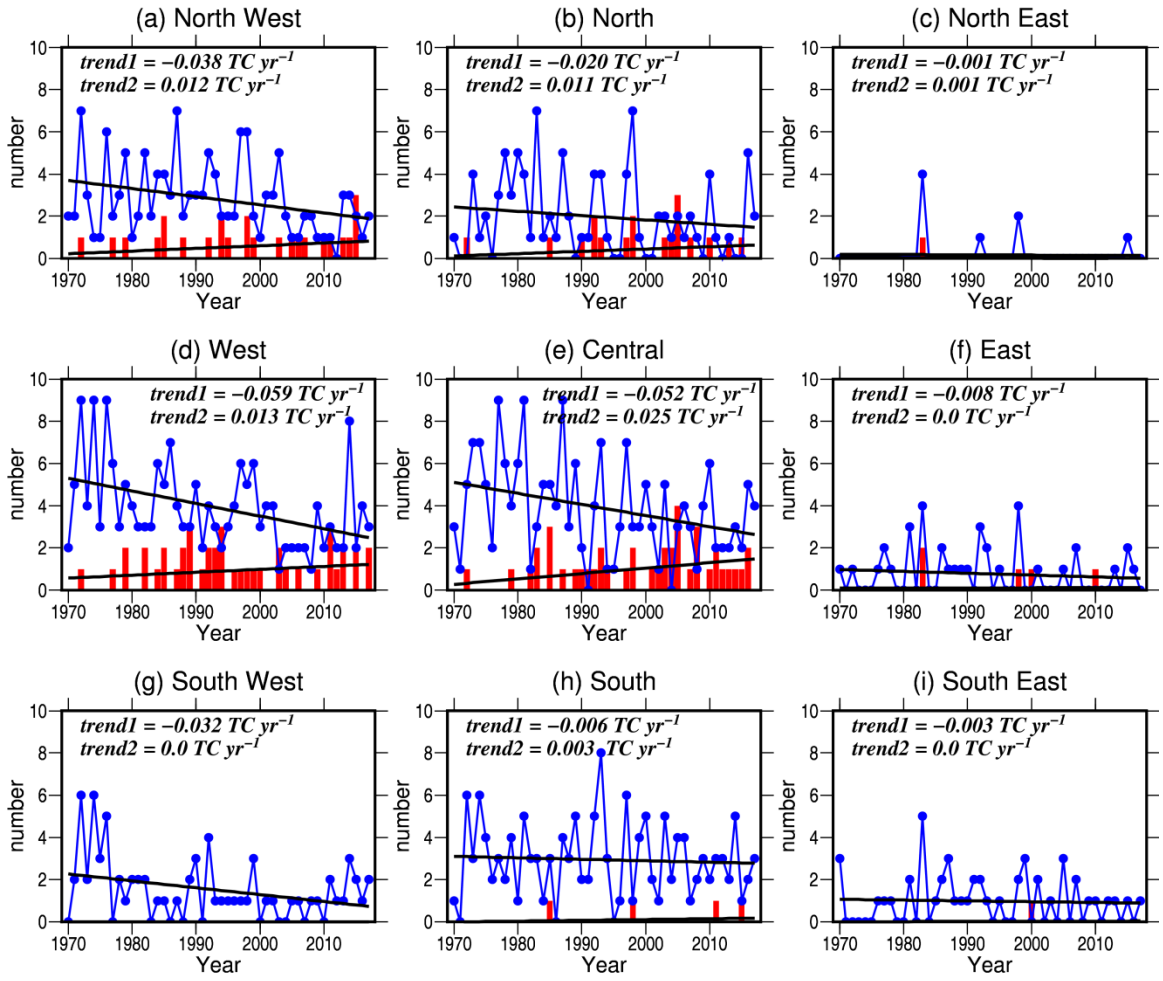

Fig. 6. Interannual variation in the number of TCs over the study subdomains. The blue dots represent weaker TCs and red bars represent stronger TCs. The numbers indicate the slopes of the linear trends of weaker TCs (trend1) and stronger TCs (trend2).

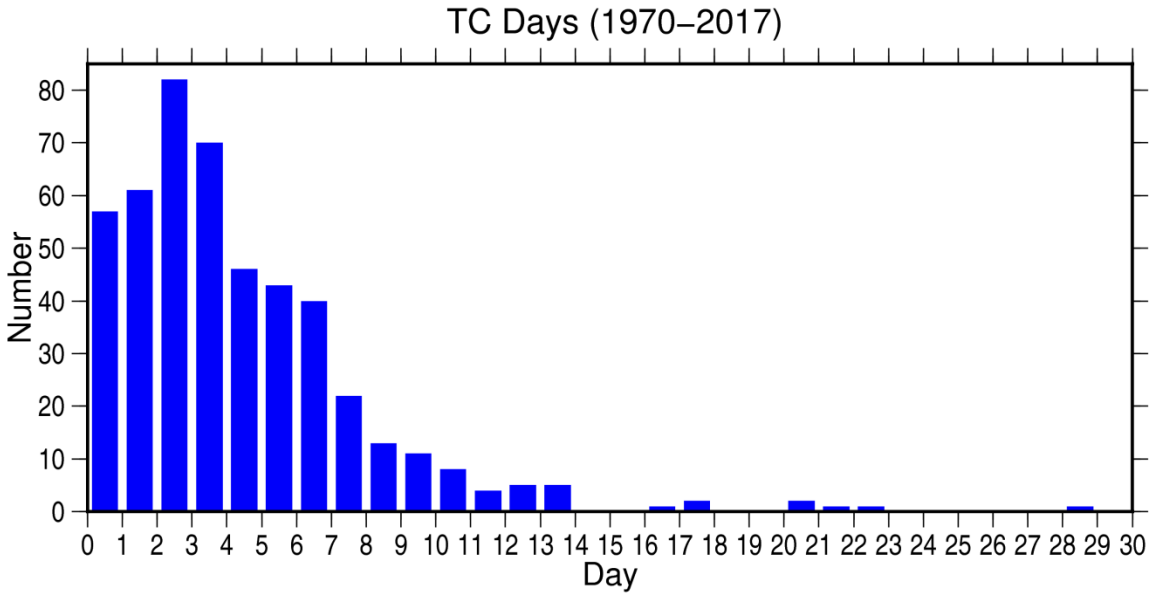

Fig. 7. Histogram showing frequency of TC lifetimes during 1970–2017.

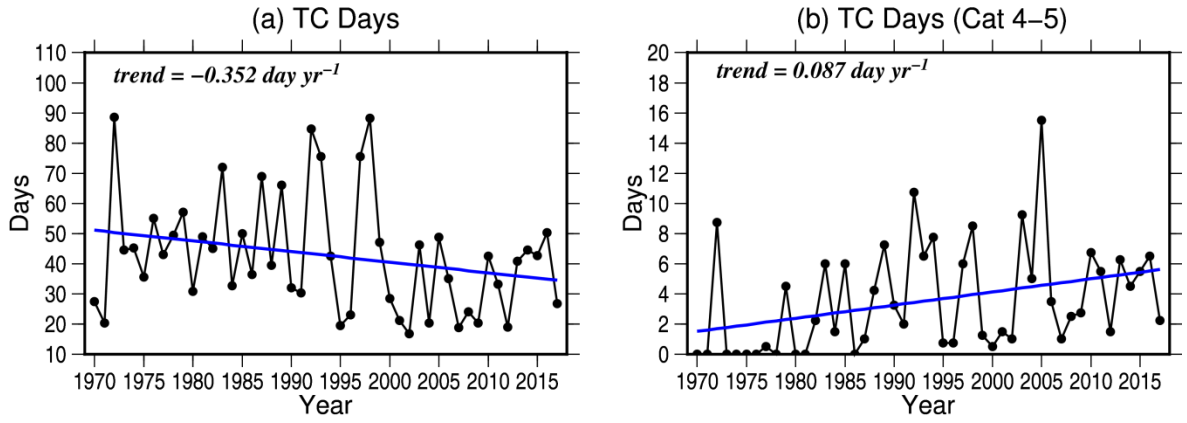

Fig. 8. Interannual variation in total TC days during 1970–2017. (a) Total TC days for all TCs, (b) total TC days of stronger TCs (category 4–5; $V \geq 86$ knots). The numbers indicate the slope of the linear trend.

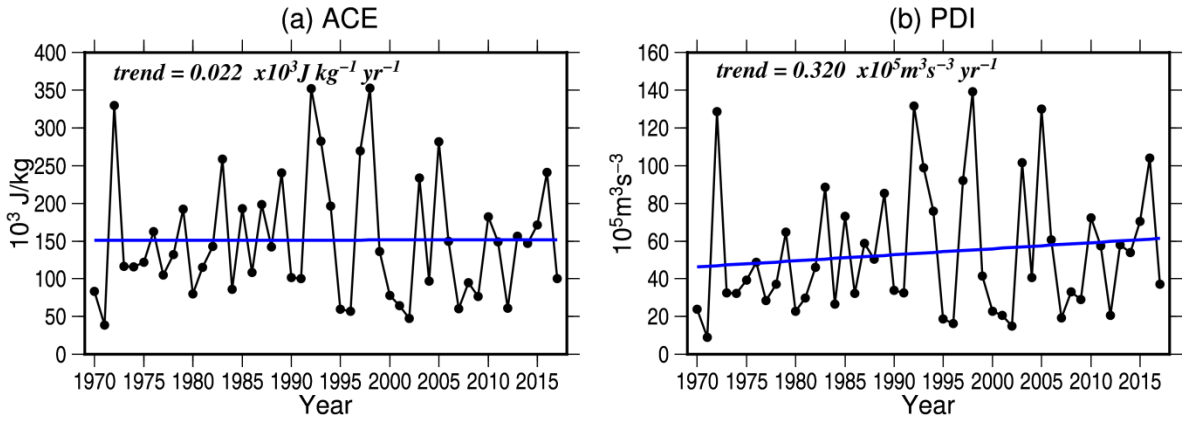

Fig. 9. Interannual variation in (a) ACE (J kg^{-1}) and (b) PDI (m^3 s^{-3}) during 1970–2017. The numbers indicate the slope of the linear trend.

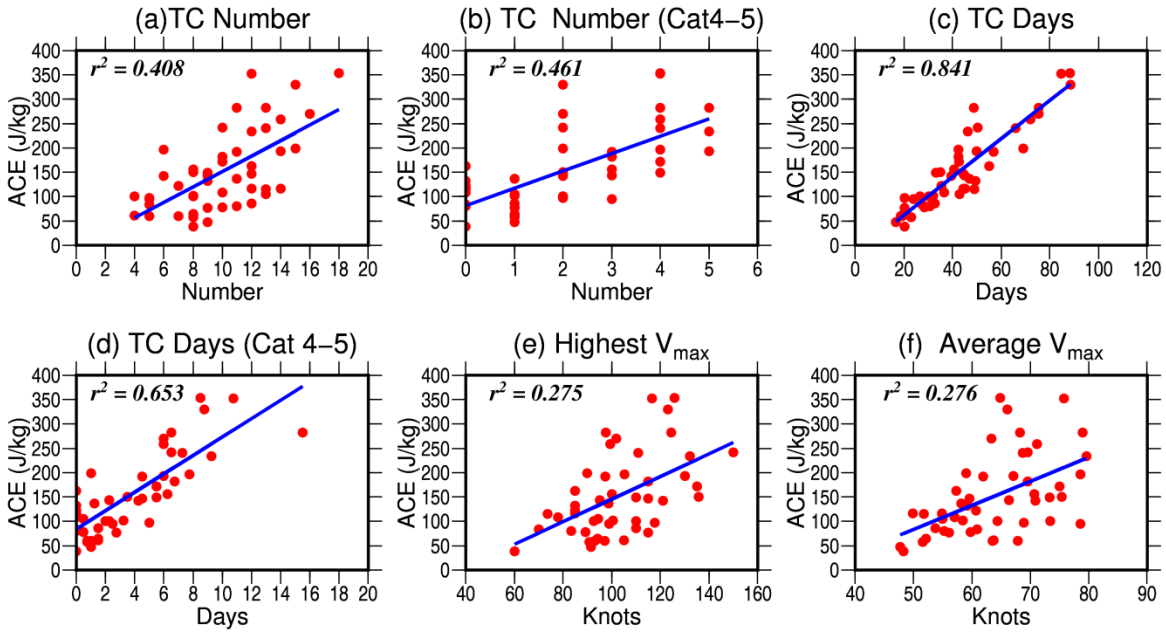

Fig. 10. Scatter plots of ACE versus (a) TC number, (b) stronger TC number, (c) TC days, (d) stronger TC days, (e) highest annual lifetime-maximum TC intensity ($\hat{V}_{max}$) and (f) average annual V_{max} ($\bar{V}_{max}$). The blue lines indicate the linear trend, and the numbers indicate the coefficients of determination.

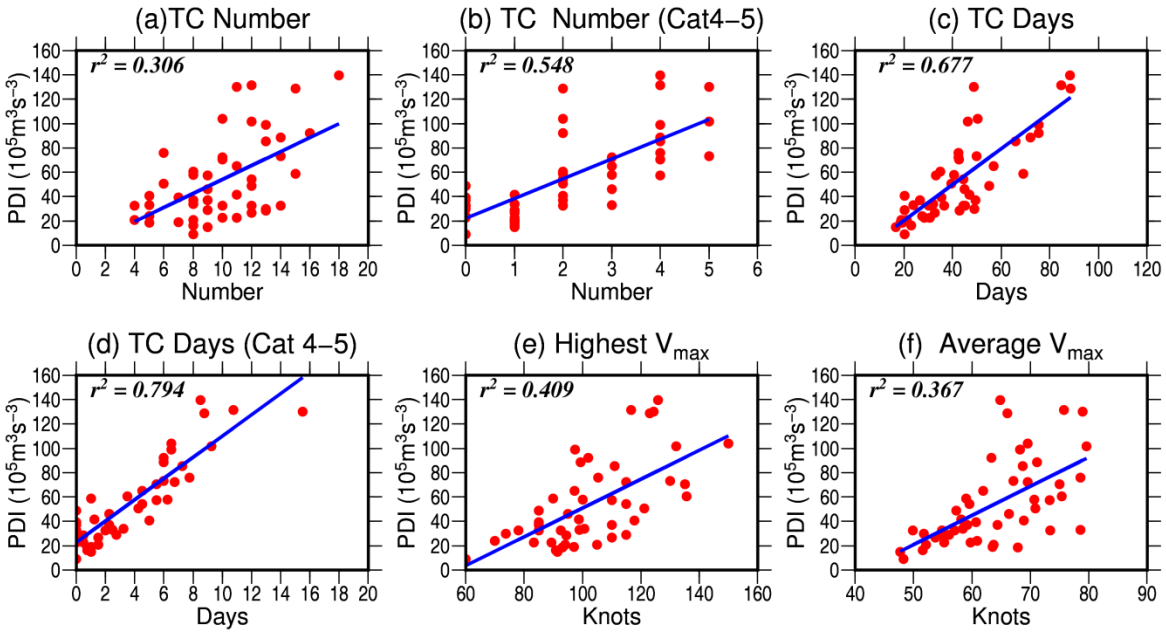

Fig. 11. Scatter plots of PDI versus (a) TC number, (b) stronger TC number, (c) TC days, (d) stronger TC days, (e) highest annual lifetime-maximum TC intensity ($\hat{V}_{max}$) and (f) average annual V_{max} ($\bar{V}_{max}$). The blue lines indicate linear trends, and the numbers indicate the coefficients of determination.

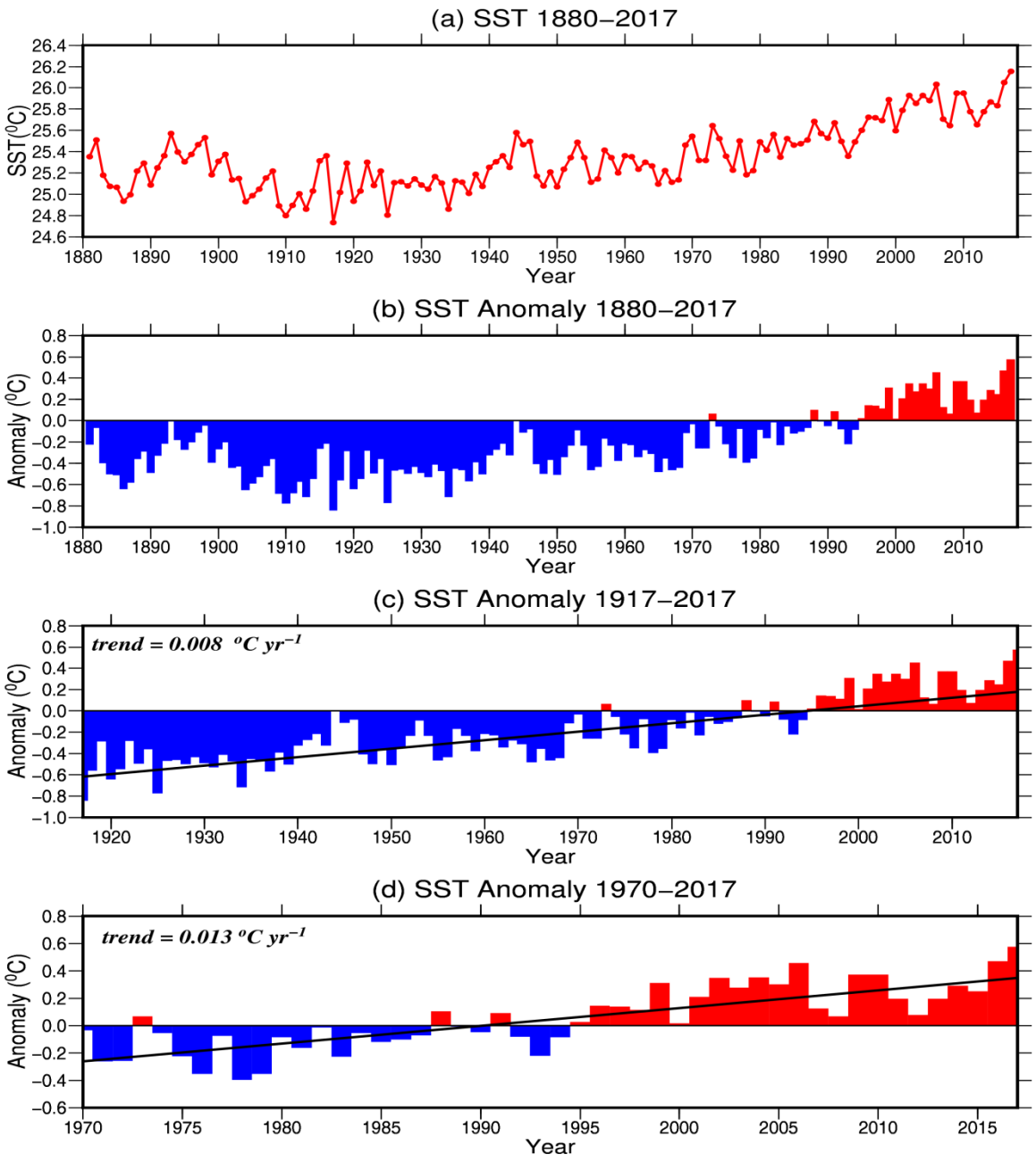

Fig. 12. Time variations of annual average SST. (a) SST time series 1880–2017, (b) SST anomaly time series 1880–2017, (c) SST anomaly time series 1917–2017, and (d) SST anomaly time series 1970–2017. The red bars represent positive anomalies, and the blue bars represent negative anomalies. The numbers represent the slope of the linear trends.

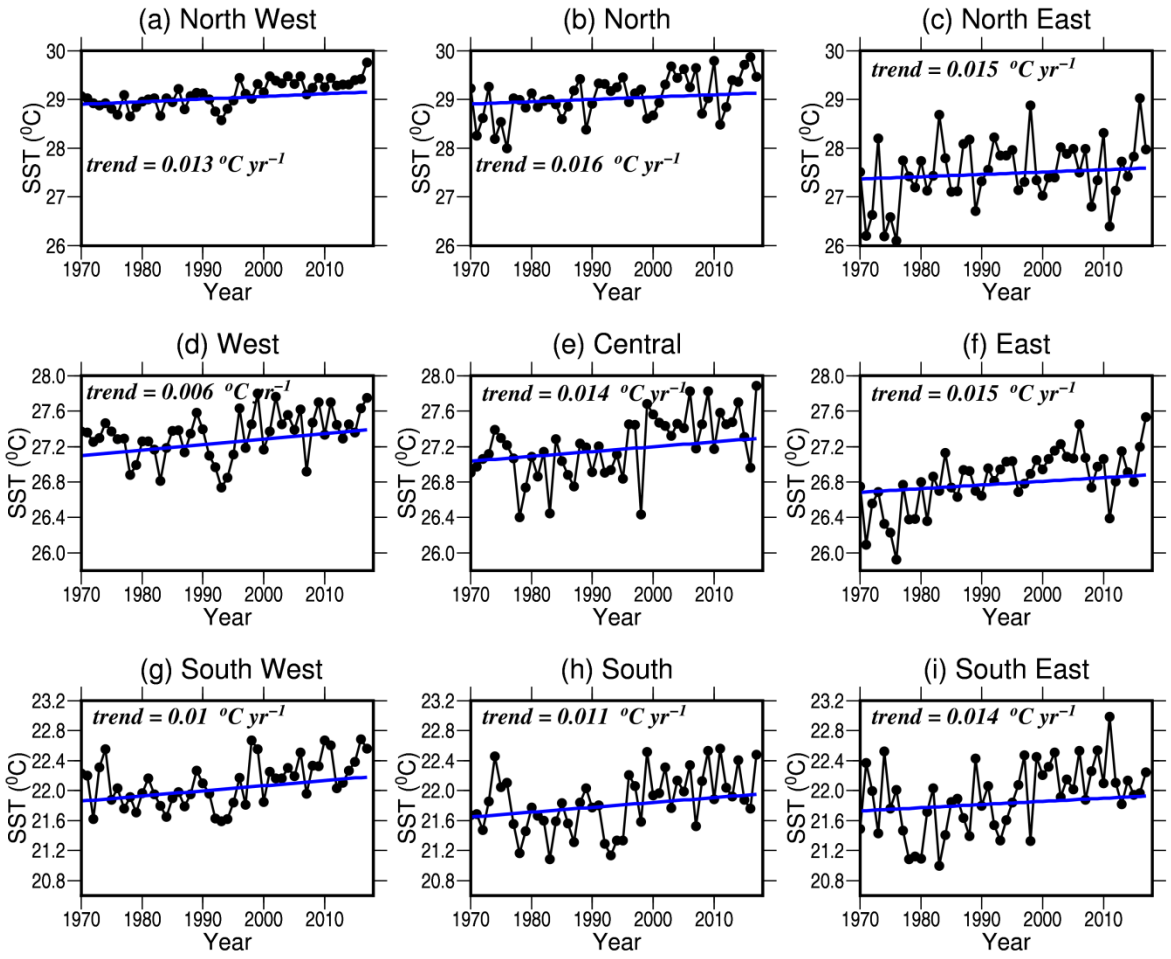

Fig. 13. Interannual variations in SST during 1970–2017 over subdomains of the Southwest Pacific. The blue lines represent linear trends, and the numbers quantify the trends.

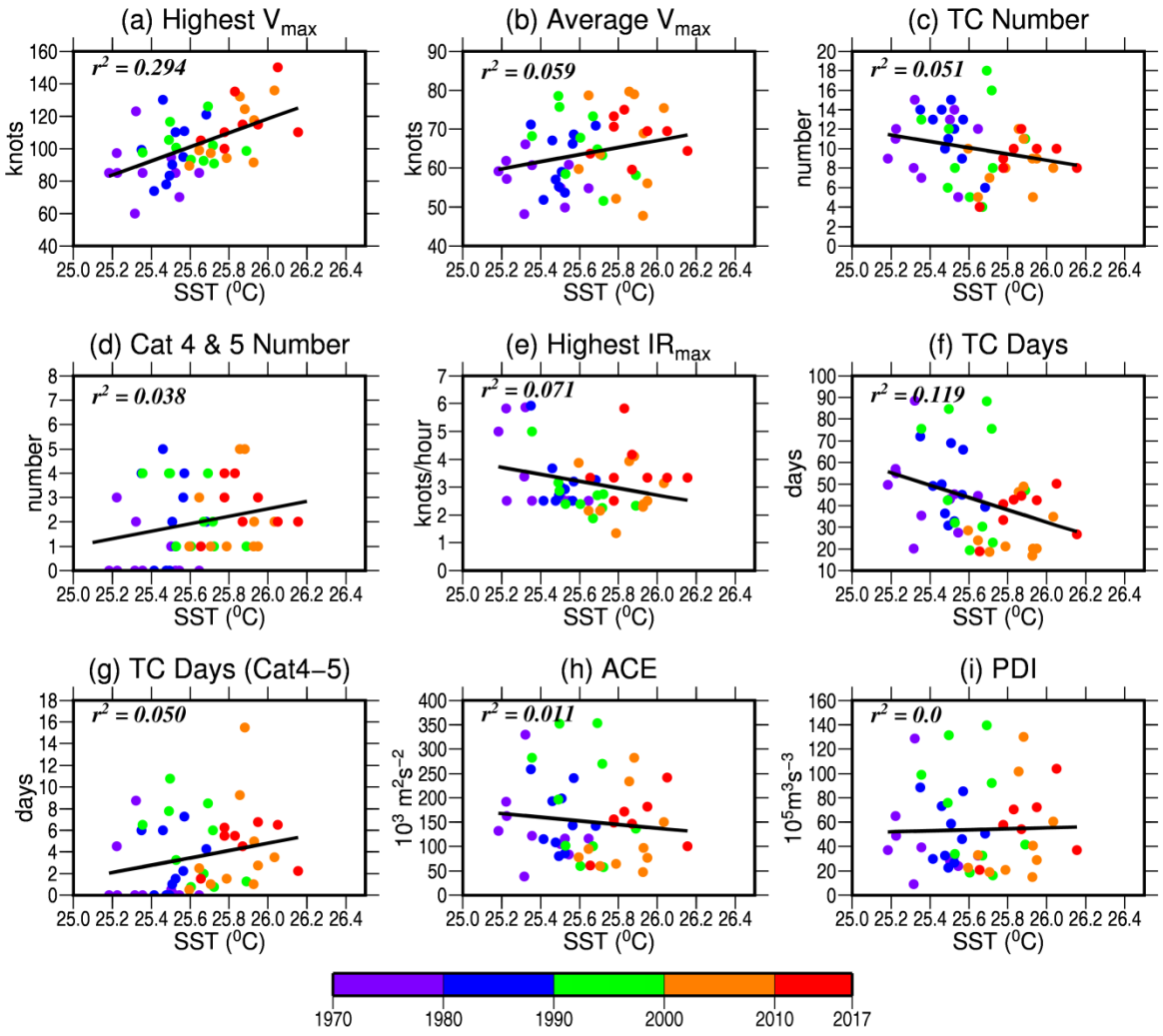

Fig. 14. Relationship between TC metrics and SST during 1970–2017. (a) highest annual lifetime-maximum intensity ($\hat{V}_{max}$), (b) average annual V_{max} ($\bar{V}_{max}$), (c) number of TCs, (d) number of stronger TCs (Cat 4–5), (e) highest annual maximum intensification rate ($\widehat{IR}_{max}$), (f) number of TC days, (g) number of stronger TC days (Cat 4–5), (h) ACE, and (i) PDI. The black lines show linear trend, and the numbers indicate the coefficients of determination. The color scale represents the time period of data points.

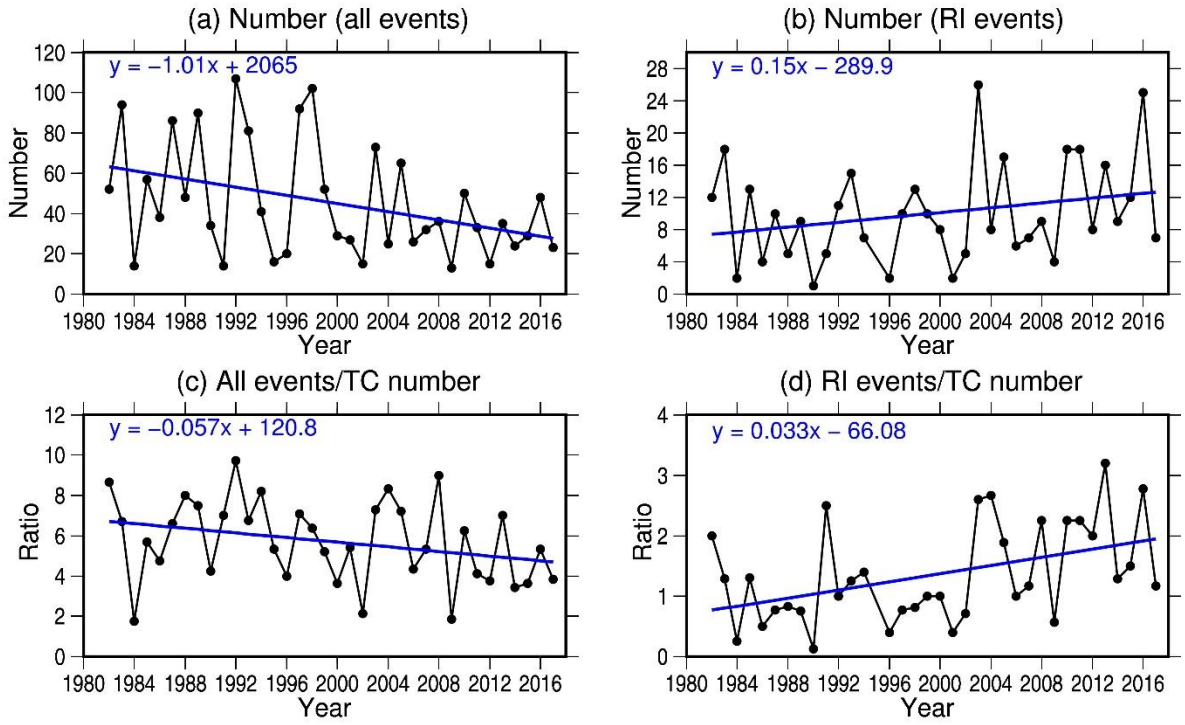

Fig. 15. Interannual variation in the number of intensifying events during 1982-2017. (a) Number of all intensifying events for the entire SWP, and (b) number of rapidly intensifying events. (c) The time series of the ratio of intensifying events to TC number, and (d) the ratio of RI event to TC number. The blue lines show the linear trends, and their expressions are shown in the top left corner of each panel.

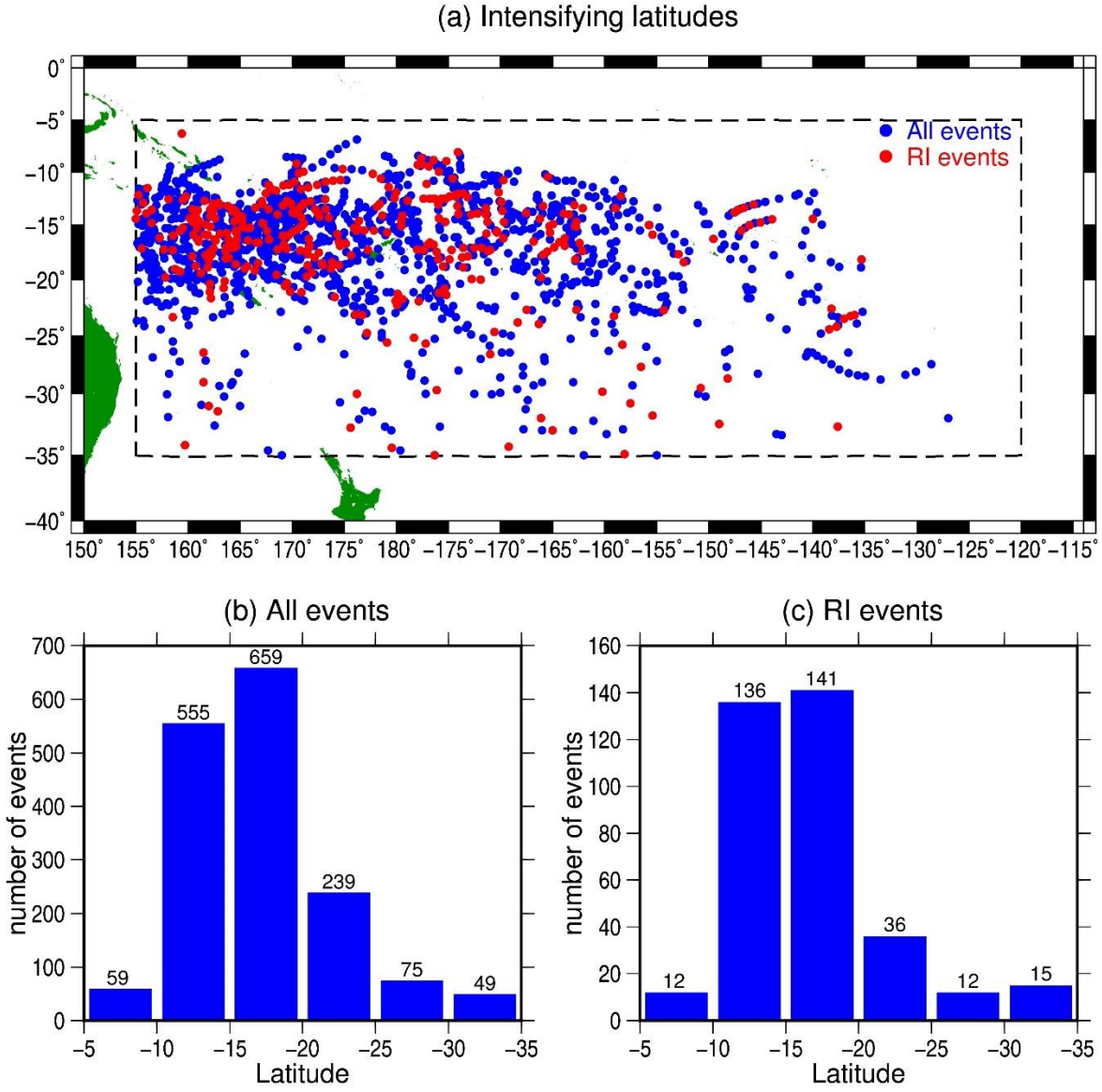

Fig. 16. (a) Spatial location of tropical cyclone (TC) intensifying location for all events (blue) and for rapidly intensifying (RI) events (red) for the period 1982-2017. (b) Histogram showing frequency distribution (1982-2017) of intensifying location for all events, and (c) those for RI events.

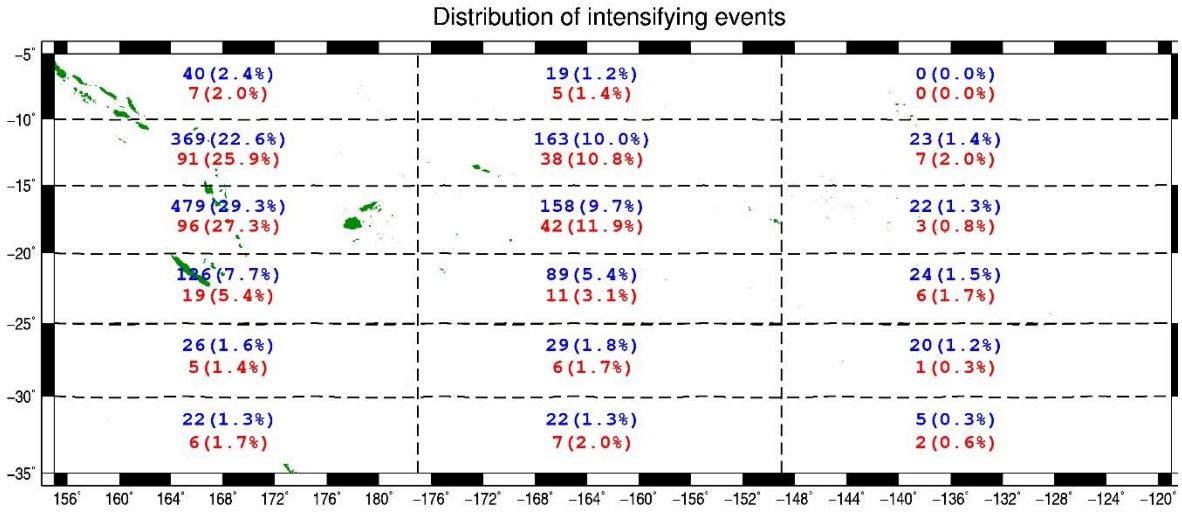

Fig. 17. Number and percentage (in brackets) of intensifying events (blue letters) and rapidly intensifying events (red letters) in the subdomains (represent by dashed lines) of the study domain.

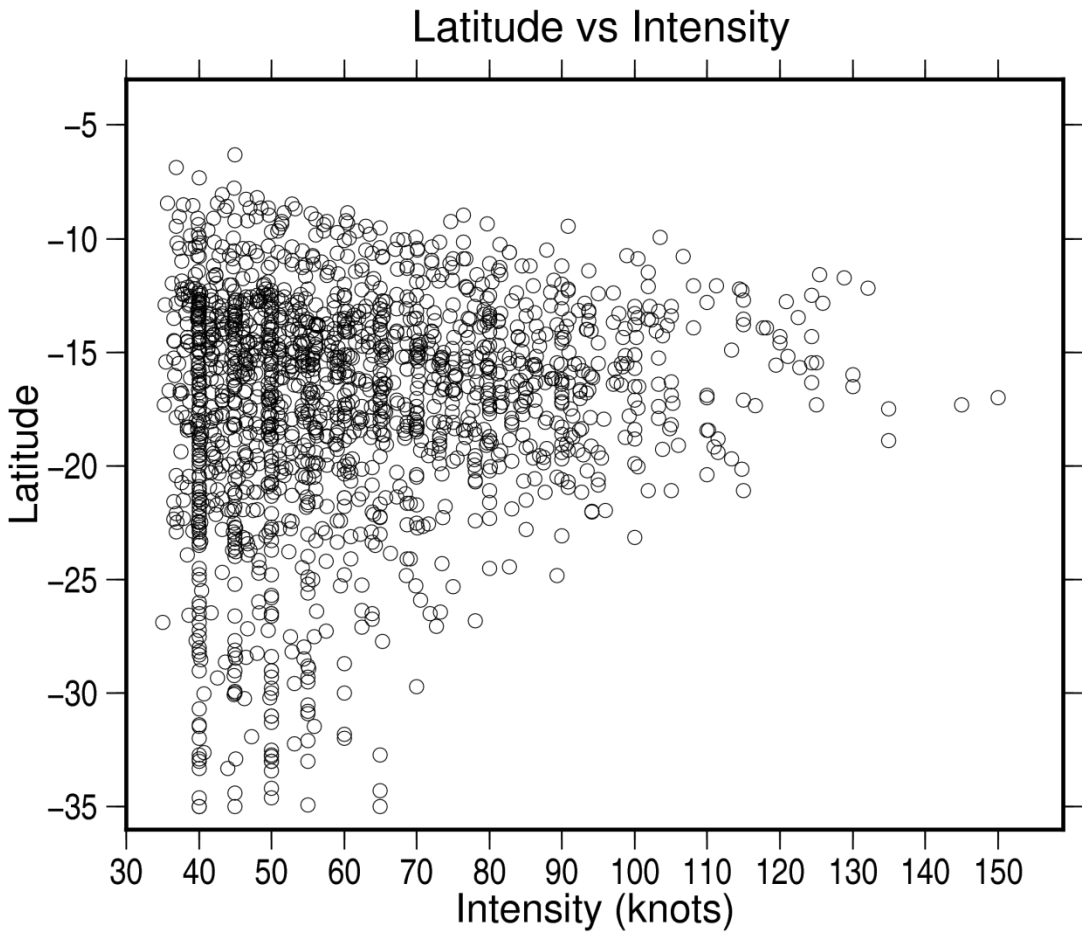

Fig. 18. Scatter diagram of intensifying location against current TC intensity from 1982 to 2017

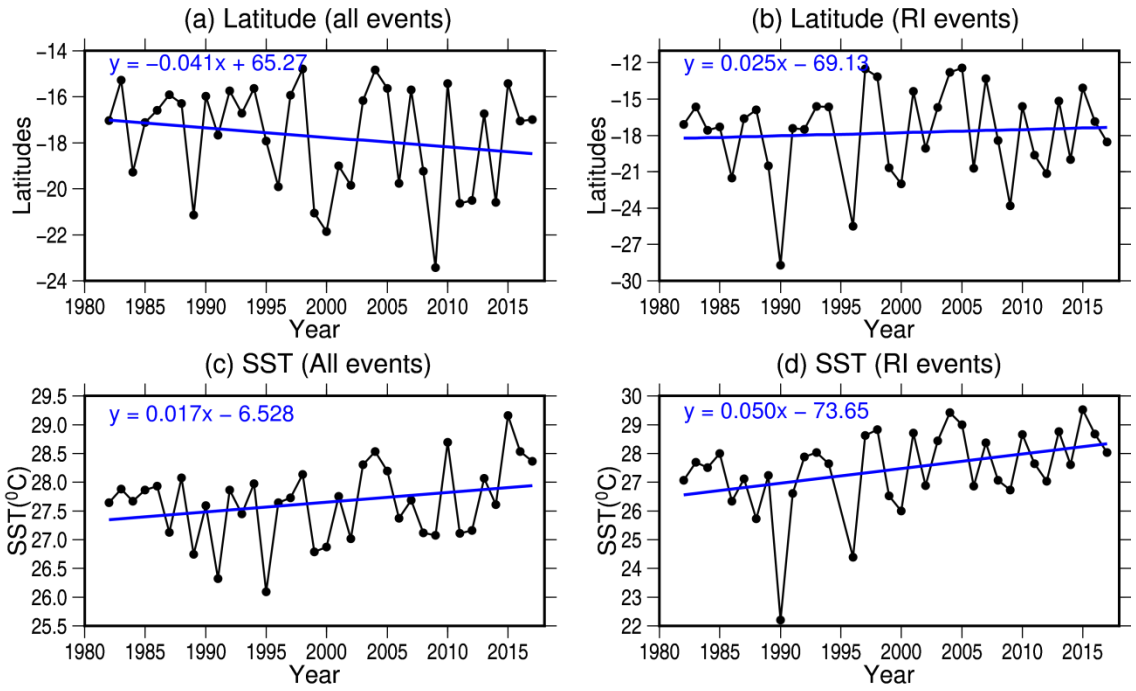

Fig. 19. Time series of the annual average latitude of intensification (a) all intensifying events, (b) rapidly intensifying events and for SST at point of intensification for (c) all intensifying events, and (d) rapidly intensifying events. The blue lines show the linear trend, and their expressions are shown in the top left corner of each panel.

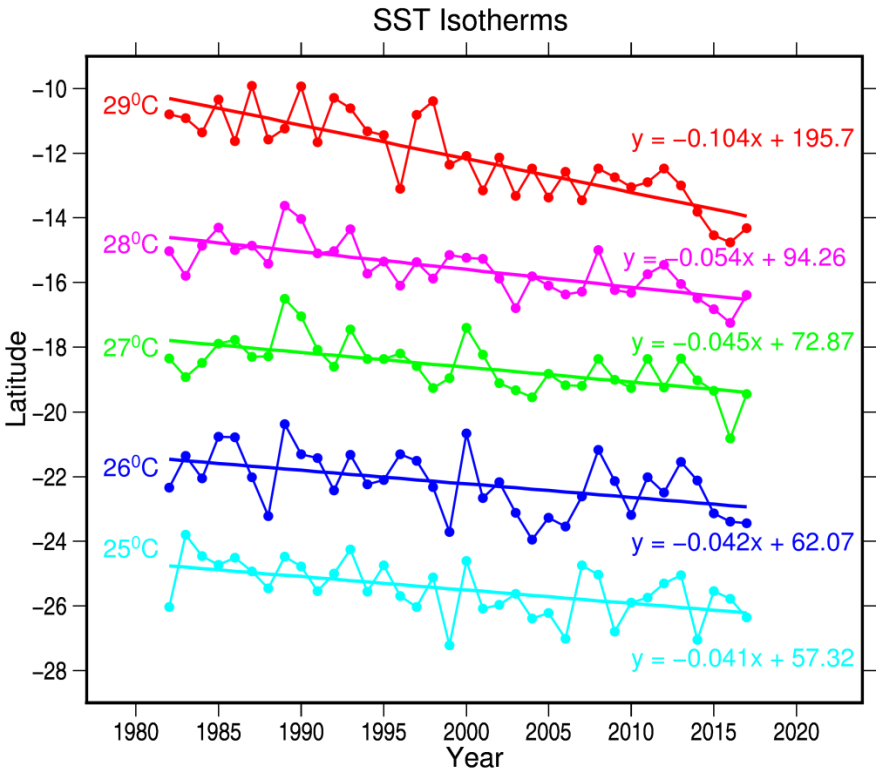

Fig. 20. Time series of the annual average position of SST isotherms based on the OISST dataset. The expressions near each line represent the slope.

Tables

TABLE 1: The number of TCs in the Southwest Pacific by decade for the period 1970–2017. Intensities are based on the Australia Intensity scale (http://www.bom.gov.au/cyclone/about/intensity.shtml).

Period	TCs	Weaker TCs < 86knots	Stronger TCs ≥86knots	TC Days	Weaker TC Days	Stronger TC Days
1970-1979	106	100	6	466.0	452.25	13.75
1980-1989	117	96	21	490.5	462.25	28.25
1990-1999	101	77	24	518.25	470.75	47.5
2000-2009	84	62	22	279.75	237.25	42.5
2010-2017	71	50	21	299.75	261.0	38.75
TOTAL	**479**	**385**	**94**	**2054.25**	**1883.5**	**170.75**
Average (TCs yr^{-1})	**9.98**	**8.02**	**2.02**	**42.8**	**39.24**	**3.56**

TABLE 2. The annual maximum intensification rates ($\widehat{IR}_{max}$). V_{n-1} and V_n are the wind speeds involved. The asterisks (*) indicate $\widehat{IR}_{max}$ values ≥ 4.0 knots h^{-1} or 24.0 knots/6 h. Bold italics denote TCs that skipped an intensity category.

Year	V_{n-1}	V_n	IR_{max} (knots/6hr)
1970	40.0	55.0	15.0
1971	39.4	59.7	20.3
1972	70.4	105.6	35.2*
1973	40.0	55.0	15.0
1974	40.0	55.0	15.0
1975	40.0	55.0	15.0
1976	40.0	55.0	15.0
1977	59.3	75.2	15.9
1978	***40.0***	***70.0***	***30.0****
1979	50.0	85.0	35.0*
1980	39.7	55.9	16.2
1981	40.0	55.0	15.0
1982	65.0	80.0	15.0
1983	***35.2***	***70.8***	***35.6****
1984	74.8	92.4	17.6
1985	***45.7***	***67.7***	***22.0***
1986	40.0	55.0	15.0
1987	37.1	55.0	17.9
1988	40.5	60.0	19.5
1989	73.4	92.6	19.2
1990	45.7	60.0	14.3
1991	61.1	72.4	11.3
1992	81.2	98.4	17.2
1993	***60.0***	***90.0***	***30.0****
1994	41.0	60.0	19.0
1995	58.5	72.8	14.3
1996	49.2	65.7	16.5
1997	78.2	91.7	13.5
1998	101.9	118.1	16.2
1999	36.0	50.0	14.0
2000	***42.5***	***65.7***	***23.2***
2001	62.4	70.5	8.1
2002	35.4	49.2	13.8
2003	101.9	125.5	23.6
2004	103.3	117.7	14.4
2005	51.3	76.0	24.7*
2006	78.0	96.8	18.8
2007	42.8	55.7	12.9
2008	52.1	65.0	12.9
2009	35.0	50.0	15.0
2010	80.0	100.0	20.0
2011	70.0	90.0	20.0
2012	70.0	90.0	20.0
2013	65.0	80.0	15.0
2014	***85.0***	***110.0***	***25.0****
2015	50.0	85.0	35.0*
2016	60.0	80.0	20.0
2017	35.0	55.0	20.0

TABLE 3: Number of TCs, number of intensifying events and intensifying location in the SWP by decade for the period 1982-2017. Average numbers per year are indicated in parentheses.

Year	**TC number**	**Number of Events**		**Average Latitude of Events**	
		All	**RI**	**All**	**RI**
1982-1991	87 (8.7)	527 (52.7)	79 (7.9)	-17.16	-17.45
1992-2001	88 (8.8)	567 (56.7)	78 (7.8)	-16.90	-16.60
2002-2011	68 (6.8)	368 (36.8)	118 (11.8)	-17.21	-16.35
2012-2017	39 (6.5)	174 (29.0)	77 (12.8)	-17.49	-17.03
TOTAL	**282**	**1636**	**352**	**-**	**-**
AVERAGE	**7.80**	**45.44**	**9.80**	**-17.19**	**-16.80**

List of Published/Submitted papers

Tauvale L., and K. Tsuboki, 2019: Characteristics of tropical cyclones in the Southwest Pacific. *J. Meteor. Soc. Japan*, **97**, 711–731, doi:10.2151/jmsj.2019-042. (Published on April 1, 2019).

Tauvale, L., and K. Tsuboki, 2019: Climatological Aspects of Tropical Cyclone Intensifying Latitude in the Southwest Pacific. *SOLA* (In Press, submitted on December 11, 2019).